

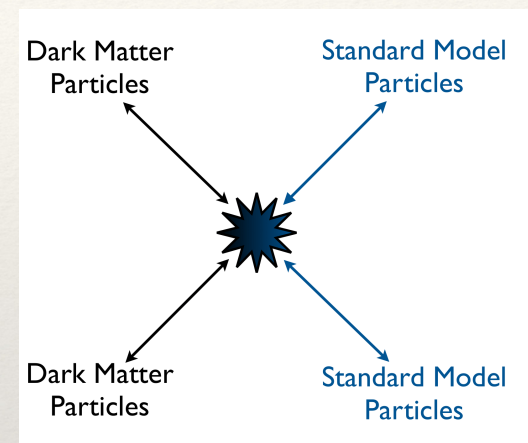
Dark Matter Indirect Detections

- ❖ Kenny CY Ng
- ❖ kcyng@cuhk.edu.hk
- ❖ Sci Cen North Black 345
- ❖ CUHK
- ❖ Course webpage: <https://blackboard.cuhk.edu.hk>



Indirect detection

- ❖ To look for the presence of dark matter interactions in remote locations
- ❖ WIMPs
 - ❖ They can annihilate into standard model particles
- ❖ Axions
 - ❖ Some axion dark matter can decay into photons
- ❖ Sterile neutrinos
 - ❖ The sterile-active mixing makes the sterile neutrino decay
- ❖ Primordial black holes
 - ❖ Light PBHs emit radiation via hawking radiation



Dark Matter annihilation

- ❖ Let's talk about dark matter annihilation first
- ❖ A definite prediction of WIMPs
- ❖ $\langle \sigma v \rangle \sim 3 \times 10^{-26} \text{ cm}^3/\text{s}$
- ❖ Consider a gas of dark matter particle with density ρ_χ , mass m_χ
- ❖ If dark matter is its own antiparticle, the rate of dark matter self-annihilation in the volume is
- ❖
$$\frac{1}{2} \left(\frac{\rho_\chi}{m_\chi} \right)^2 \sigma v dV$$
 - ❖ [Number per time]
- ❖ The 1/2 factor take into account double counting
- ❖ If dark matter is symmetric (equal dark and anti dark matter), then it is $(\frac{1}{2} \frac{\rho_\chi}{m_\chi})^2 \sigma v dV$

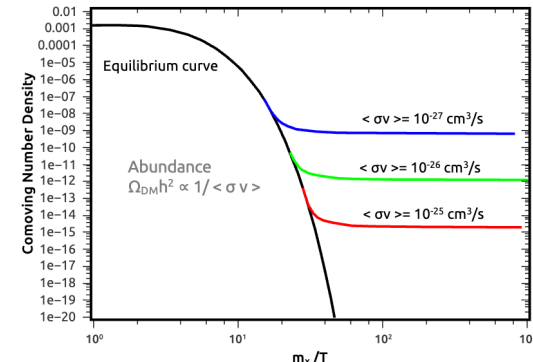


FIG. 1. Comoving number density evolution as a function of the ratio m_χ/T in the context of the thermal freeze-out. Notice that the size of the annihilation cross section determines the DM abundance since $\Omega_{DM} \propto 1/\langle \sigma v \rangle$.

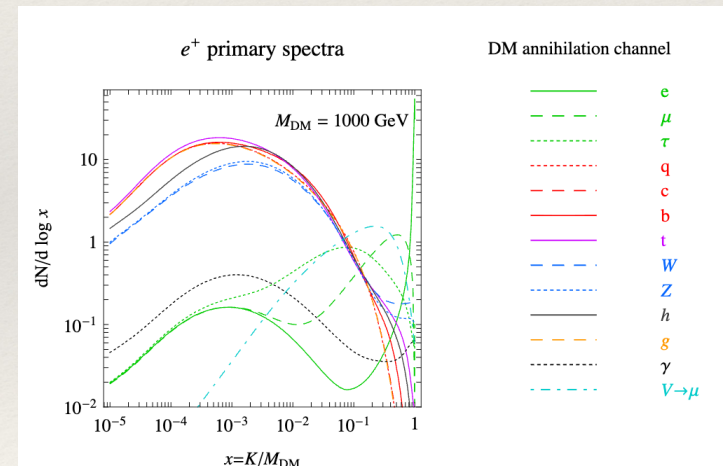
Annihilation channels

- ❖ Let's assume that per annihilation, the output particle spectrum is given by $\frac{dN_i}{dE}$
- ❖ We care about things that can be used to detect this interactions, so i could be
 - ❖ Electron/positrons, photons, neutrinos, etc
 - ❖ It can also first annihilate unstable particles, like quarks
 - ❖ They can further decay into astrophysical messengers
- ❖ So, as you can see, we have to specify the annihilation “channel”. E.g.,
 - ❖ $\chi\chi \rightarrow b\bar{b}$
 - ❖ The branching fraction is the fraction of a specific channel
 - ❖ They summed up to the total cross section
 - ❖ $\sigma v = \sigma v \sum_i Br_i$

PPPC 4 DM ID: A Poor Particle Physicist Cookbook for Dark Matter Indirect Detection

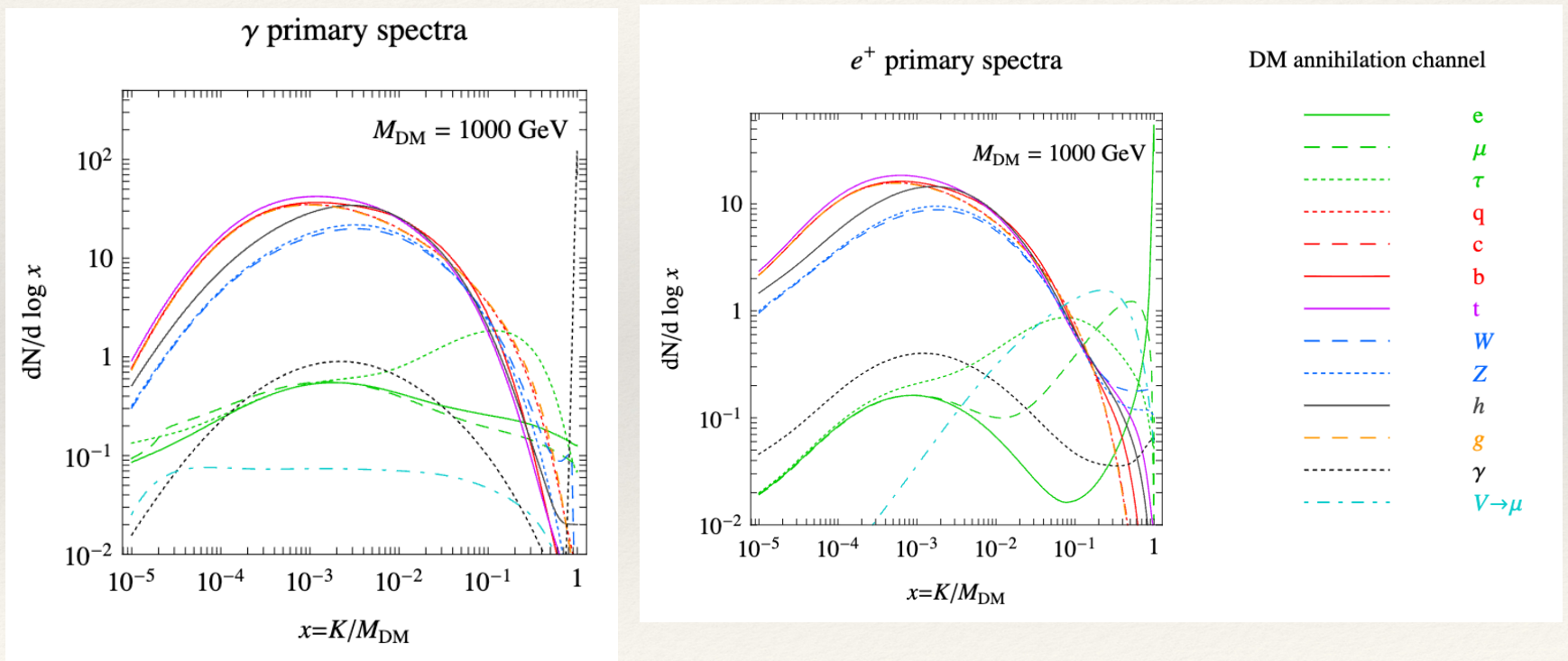
Marco Cirelli, Gennaro Corcella, Andi Hektor, Gert Hütsi, Mario Kadastik, Paolo Panci, Martti Raidal, Filippo Sala, Alessandro Strumia

We provide ingredients and recipes for computing signals of TeV-scale Dark Matter annihilations and decays in the Galaxy and beyond. For each DM channel, we present the energy spectra of electrons and positrons, antiprotons, antideuterons, gamma rays, neutrinos and antineutrinos e, mu, tau at production, computed by high-statistics simulations. We estimate the Monte Carlo uncertainty by comparing the results yielded by the Pythia and Herwig event generators. We then provide the propagation functions for charged particles in the Galaxy, for several DM distribution profiles and sets of propagation parameters. Propagation of electrons and positrons is performed with an improved semi-analytic method that takes into account position-dependent energy losses in the Milky Way. Using such propagation functions, we compute the energy spectra of electrons and positrons, antiprotons and antideuterons at the location of the Earth. We then present the gamma ray fluxes, both from prompt emission and from Inverse Compton scattering in the galactic halo. Finally, we provide the spectra of extragalactic gamma rays. All results are available in numerical form and ready to be consumed.



Annihilation Spectrum

- ❖ Example annihilation spectra for various channels



S-wave, p-wave, etc

<https://arxiv.org/pdf/1211.7090.pdf>

- ❖ WIMPs production predicted
 - ❖ $\langle \sigma v \rangle \sim 3 \times 10^{-26} \text{ cm}^3/\text{s}$
- ❖ Is this the same as σv in the annihilation calculation?
 - ❖ $\frac{1}{2} \left(\frac{\rho_\chi}{m_\chi} \right)^2 \sigma v dV ??$
- ❖ =====
- ❖ This depends on the underlying dark matter theory
- ❖

To define a representative set of models, assume that the WIMP couples only to standard model fermions. For a scalar WIMP, the interactions between the WIMP, represented by the field ϕ , and a fermion, represented by f , are

$$\text{Scalar} \quad \frac{F_S}{\sqrt{2}} \bar{\phi} \phi \bar{f} f, \quad (63)$$

$$\text{Vector} \quad \frac{F_V}{\sqrt{2}} \bar{\phi} \overleftrightarrow{\partial}_\mu \phi \bar{f} \gamma^\mu f, \quad (64)$$

$$\text{Scalar-Pseudoscalar} \quad \frac{F_{SP}}{\sqrt{2}} \bar{\phi} \phi \bar{f} \gamma_5 f, \quad (65)$$

$$\text{Vector-axialvector} \quad \frac{F_{VA}}{\sqrt{2}} (\bar{\phi} \overleftrightarrow{\partial}_\mu \phi) \bar{f} \gamma^\mu \gamma_5 f. \quad (66)$$

For fermionic WIMPs, represented by χ , the corresponding interactions are

$$\text{Scalar} \quad \frac{G_S}{\sqrt{2}} \bar{\chi} \chi \bar{f} f \quad (67)$$

$$\text{Pseudoscalar} \quad \frac{G_P}{\sqrt{2}} \bar{\chi} \gamma^5 \chi \bar{f} \gamma_5 f \quad (68)$$

$$\text{Vector} \quad \frac{G_V}{\sqrt{2}} \bar{\chi} \gamma^\mu \chi \bar{f} \gamma_\mu f \quad (69)$$

$$\text{Axialvector} \quad \frac{G_A}{\sqrt{2}} \bar{\chi} \gamma^\mu \gamma^5 \chi \bar{f} \gamma_\mu \gamma_5 f \quad (70)$$

$$\text{Tensor} \quad \frac{G_T}{\sqrt{2}} \bar{\chi} \sigma^{\mu\nu} \chi \bar{f} \sigma_{\mu\nu} f. \quad (71)$$

S-wave, p-wave, etc

<https://arxiv.org/pdf/1211.7090.pdf>

- ❖ WIMPs production predicted
 - ❖ $\langle \sigma v \rangle \sim 3 \times 10^{-26} \text{ cm}^3/\text{s}$
- ❖ Is this the same as σv in the annihilation calculation?
 - ❖ $\frac{1}{2}(\frac{\rho_\chi}{m_\chi})^2 \sigma v dV ??$
- ❖ =====
- ❖ This depends on the underlying dark matter theory
- ❖ For non-relativistic dark matter annihilation, the cross section is parametrised as
- ❖ $\sigma v \simeq a + bv^2$
- ❖ The first term is called s-wave, second term p-wave, etc.
- ❖ If dark matter is annihilation is s-wave, then $\langle \sigma v \rangle = \sigma v$
 - ❖ If p-wave, it is suppressed by v^2 , with v being about 10^{-3} c in the galactic halo
 - ❖ Most people only consider s-wave for realistic detection.

From the interactions above it is possible to define the annihilation cross sections, and expand them as $\sigma_{\text{ann}} v \simeq a + bv^2$. For scalar dark matter these are given by [\(Beltran et al., 2009; Zheng et al., 2012; Yu et al., 2012\)](#)

$$(\sigma_{\text{ann}} v)_S \simeq \frac{1}{4\pi} \left(\frac{F_S}{\sqrt{2}} \right)^2 c_f \left(1 - \frac{m_f^2}{M_{dm}^2} \right)^{3/2} \quad (72)$$

$$(\sigma_{\text{ann}} v)_V \simeq \frac{1}{2\pi} \left(\frac{F_V}{\sqrt{2}} \right)^2 c_f M_{dm}^2 \frac{1}{3} \sqrt{1 - \frac{m_f^2}{M_{dm}^2}} \left(2 + \frac{m_f^2}{M_{dm}^2} \right) v^2, \quad (73)$$

$$(\sigma_{\text{ann}} v)_{SP} \simeq \frac{1}{4\pi} \left(\frac{F_{SP}}{\sqrt{2}} \right)^2 c_f \sqrt{1 - \frac{m_f^2}{M_{dm}^2}} \quad (74)$$

$$(\sigma_{\text{ann}} v)_{VA} \simeq \frac{1}{\pi} \left(\frac{F_{VA}}{\sqrt{2}} \right)^2 c_f \frac{1}{3} M_{dm}^2 \left(1 - \frac{m_f^2}{M_{dm}^2} \right)^{3/2} v^2 \quad (75)$$

and for fermionic dark matter,

$$(\sigma_{\text{ann}} v)_S \simeq \frac{1}{8\pi} \left(\frac{G_S}{\sqrt{2}} \right)^2 c_f \left(1 - \frac{m_f^2}{M_{dm}^2} \right)^{3/2} M_{dm}^2 v^2 \quad (76)$$

$$(\sigma_{\text{ann}} v)_P \simeq \frac{1}{2\pi} \left(\frac{G_P}{\sqrt{2}} \right)^2 c_f \sqrt{1 - \frac{m_f^2}{M_{dm}^2}} M_{dm}^2 \quad (77)$$

$$(\sigma_{\text{ann}} v)_V \simeq \frac{1}{2\pi} \left(\frac{G_V}{\sqrt{2}} \right)^2 c_f \sqrt{1 - \frac{m_f^2}{M_{dm}^2}} (2M_\chi^2 + m_f^2) \quad (78)$$

$$(\sigma_{\text{ann}} v)_A \simeq \frac{1}{2\pi} \left(\frac{G_A}{\sqrt{2}} \right)^2 c_f m_f^2 \left(\frac{8M_{dm}^2/m_f^2 - 28 + 23m_f^2/M_{dm}^2}{24\sqrt{1 - m_f^2/M_{dm}}} v^2 \right) \quad (79)$$

$$(\sigma_{\text{ann}} v)_T \simeq \frac{2}{\pi} \left(\frac{G_T}{\sqrt{2}} \right)^2 c_f \sqrt{1 - \frac{m_f^2}{M_{dm}^2}} (M_{dm}^2 + 2m_f^2) \quad (80)$$

(81)

Annihilation theory

❖ Combining the annihilation rate and the spectrum per annihilation

❖ For a small volume element

$$\text{❖ } \epsilon \equiv \frac{1}{2} \left(\frac{\rho_\chi}{m_\chi} \right)^2 \sigma v dV \frac{dN}{dE}$$

❖ [Number per time per energy]

❖ From this we can get the flux for this small volume element at a distance of r

$$\text{❖ "Flux" } \sim \frac{\epsilon}{4\pi r^2}$$

Annihilation theory

❖ More precisely

$$\frac{dF}{dE} = \frac{1}{2} \left(\frac{\rho_\chi}{m_\chi} \right)^2 \sigma v \, dV \frac{dN}{dE} \frac{1}{4\pi r^2}$$

❖ If the volume is very small and far away, then we have

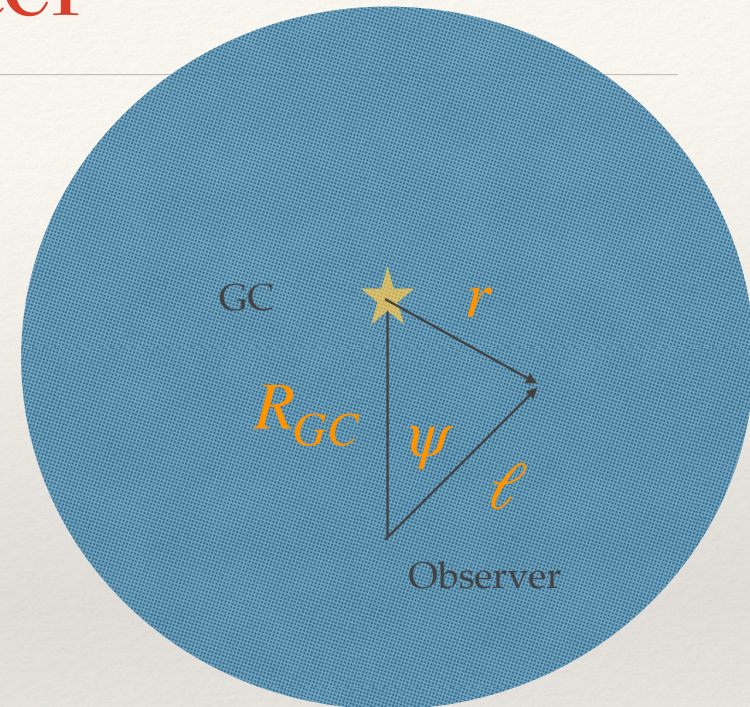
$$\frac{dF}{dE} \simeq \frac{dN}{dE} \frac{1}{4\pi r^2} \times \int \frac{1}{2} \left(\frac{\rho_\chi}{m_\chi} \right)^2 \sigma v \, dV$$

❖ Here we also assume that $\frac{dN}{dE}$ can be pulled out of the integral

Galactic Dark Matter

$$\diamond \frac{dF}{dE} = \frac{1}{2} \left(\frac{\rho_\chi}{m_\chi} \right)^2 \sigma v \, dV \frac{dN}{dE} \frac{1}{4\pi r^2}$$

- ❖ “If the volume is very small and far away”
- ❖ For annihilation inside the galactic halo, this is clearly not true. Then we should have
- ❖ $\frac{dF}{dE} = \frac{1}{2} \left(\frac{\rho_\chi}{m_\chi} \right)^2 \sigma v (\ell^2 d\ell d\Omega) \frac{dN}{dE} \frac{1}{4\pi \ell^2}$
- ❖ Changed to the line of sight distance ℓ
- ❖ Assumed the Halo is spherically symmetric $\rho = \rho(r) = \rho(r[\ell, \psi])$
- ❖ The Galacto-centric radius is related to the line of sight distance and angle (ψ) as
- ❖ $r[\ell, \psi]^2 = R_\odot^2 + \ell^2 - 2R_\odot \ell \cos \psi$
- ❖ The line of sight integral is integrated to the so called viral radius of the halo R_{vir} , as the end of the halo



Galactic Dark Matter

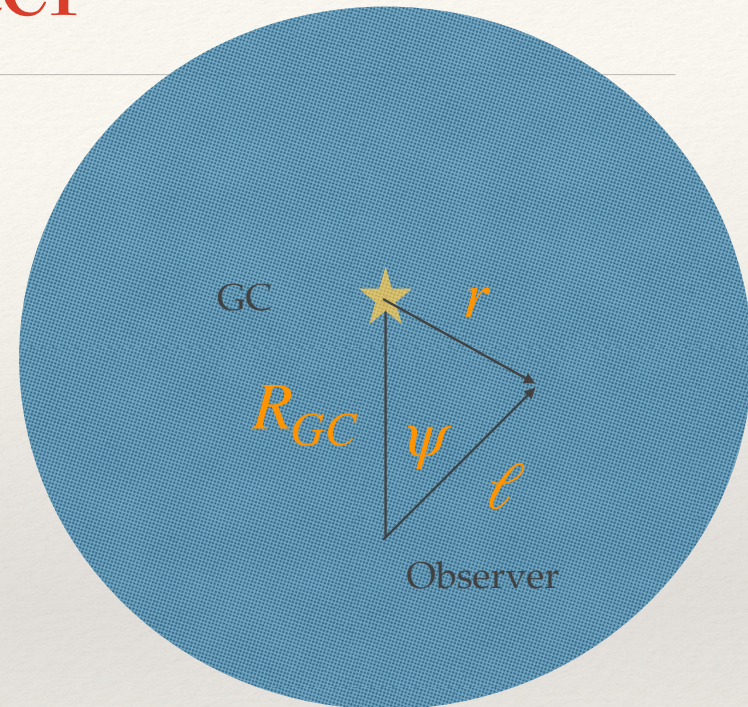
❖ Thus

$$\frac{dF}{dE} = \frac{1}{2} \left(\frac{\rho_\chi}{m_\chi} \right)^2 \sigma v (\ell^2 d\ell d\Omega) \frac{dN}{dE} \frac{1}{4\pi\ell^2}$$

$$\frac{dF}{dE} = \frac{\sigma v}{8\pi m_\chi^2} \frac{dN}{dE} \times \int d\ell d\Omega \rho_\chi^2$$

$$\text{Or } \frac{dF}{dEd\Omega} = \frac{\sigma v}{8\pi m_\chi^2} \frac{dN}{dE} \times \int d\ell \rho_\chi^2$$

- ❖ You can see that the first term depends on particle physics, but second term $\int d\ell \rho_\chi^2$, only depends on astrophysics and detector observations
- ❖ Recall that we have some idea on $\rho(r)$, e.g., NFW profile



Dark Matter annihilation search

- ❖ Now, we have these depends on the situation.

$$\frac{dF}{dE} = \frac{\sigma v}{8\pi m_\chi^2} \frac{dN}{dE} \times \int d\ell d\Omega \rho_\chi^2$$

$$\frac{dF}{dEd\Omega} = \frac{\sigma v}{8\pi m_\chi^2} \frac{dN}{dE} \times \int d\ell \rho_\chi^2$$

$$\int d\ell d\Omega \rho_\chi^2$$

- ❖ This is also commonly called the Astrophysical J-factor
- ❖ We want to look at places with large J-factors for dark matter search
 - ❖ (In practice, also low background)

Dark Matter annihilation search

- ❖ Places to search for dark matter
- ❖ For WIMPs, GeV to TeV range, so we are talking about gamma rays

- ❖ 1. Dwarf Spheroidal galaxies (satellite galaxies of MW or M31)
 - ❖ + High mass to light ratio, so high concentration of dark matter
 - ❖ + No bright gamma ray emissions
- ❖ 2. Milky Way halo, or the galactic centre
 - ❖ + close and nearby
 - ❖ - Bright gamma ray emissions
- ❖ 3. Galaxy cluster
 - ❖ + lots of dark matter
 - ❖ - far away
- ❖ 4. Cosmological dark matter search (all the dark matter in the universe, an isotropic background emission)
 - ❖ Hard to model theoretically

Fermi dark matter search with Dsphs

- ❖ Case study.
- ❖ The 2015 paper

1.HEP] 3 Nov 2015

Searching for Dark Matter Annihilation from Milky Way Dwarf Spheroidal Galaxies with Six Years of Fermi-LAT Data

M. Ackermann,¹ A. Albert,² B. Anderson,^{3, 4, *} W. B. Atwood,⁵ L. Baldini,^{6, 2} G. Barbiellini,^{7, 8} D. Bastieri,^{9, 10} K. Bechtol,¹¹ R. Bellazzini,¹² E. Bissaldi,¹³ R. D. Blandford,² E. D. Bloom,² R. Bonino,^{14, 15} E. Bottacini,² T. J. Brandt,¹⁶ J. Bregeon,¹⁷ P. Bruel,¹⁸ R. Buehler,¹ G. A. Calandro,^{2, 19} R. A. Cameron,² R. Caputo,⁵ M. Caragiulo,¹³ P. A. Caraveo,²⁰ C. Cecchi,^{21, 22} E. Charles,² A. Chekhtman,²³ J. Chiang,² G. Chiaro,¹⁰ S. Ciprini,^{24, 21, 25} R. Claus,² J. Cohen-Tanugi,¹⁷ J. Conrad,^{3, 4, 26} A. Cuoco,^{14, 15} S. Cutini,^{24, 25, 21} F. D'Ammando,^{27, 28} A. de Angelis,²⁹ F. de Palma,^{13, 30} R. Desiante,^{31, 14} S. W. Digel,² L. Di Venere,³² P. S. Drell,² A. Drlica-Wagner,^{33, †} R. Essig,³⁴ C. Favuzzi,^{32, 13} S. J. Fegan,¹⁸ E. C. Ferrara,¹⁶ W. B. Focke,² A. Franckowiak,² Y. Fukazawa,³⁵ S. Funk,³⁶ P. Fusco,^{32, 13} F. Gargano,¹³ D. Gasparrini,^{24, 25, 21} N. Giglietto,^{32, 13} F. Giordano,^{32, 13} M. Giroletti,²⁷ T. Glanzman,² G. Godfrey,² G. A. Gomez-Vargas,^{37, 38} I. A. Grenier,³⁹ S. Guiriec,^{16, 40} M. Gustafsson,⁴¹ E. Hays,¹⁶ J. W. Hewitt,⁴² D. Horan,¹⁸ T. Jogler,² G. Jóhannesson,⁴³ M. Kuss,¹² S. Larsson,^{44, 4} L. Latronico,¹⁴ J. Li,⁴⁵ L. Li,^{44, 4} M. Llena Garde,^{3, 4} F. Longo,^{7, 8} F. Loparco,^{32, 13} P. Lubrano,^{21, 22} D. Malyshev,² M. Mayer,¹ M. N. Mazziotta,¹³ J. E. McEnery,^{16, 46} M. Meyer,^{3, 4} P. F. Michelson,² T. Mizuno,⁴⁷ A. A. Moiseev,^{48, 46} M. E. Monzani,² A. Morselli,³⁷ S. Murgia,⁴⁹ E. Nuss,¹⁷ T. Ohsugi,⁴⁷ M. Orienti,²⁷ E. Orlando,² J. F. Ormes,⁵⁰ D. Paneque,^{51, 2} J. S. Perkins,¹⁶ M. Pesce-Rollins,^{12, 2} F. Piron,¹⁷ G. Pivato,¹² T. A. Porter,² S. Rainò,^{32, 13} R. Rando,^{9, 10} M. Razzano,^{12, 52} A. Reimer,^{53, 2} O. Reimer,^{53, 2} S. Ritz,⁵ M. Sánchez-Conde,^{4, 3} A. Schulz,¹ N. Sehgal,⁵⁴ C. Sgrò,¹² E. J. Siskind,⁵⁵ F. Spada,¹² G. Spandre,¹² P. Spinelli,^{32, 13} L. Strigari,⁵⁶ H. Tajima,^{57, 2} H. Takahashi,³⁵ J. B. Thayer,² L. Tibaldo,² D. F. Torres,^{45, 58} E. Troja,^{16, 46} G. Vianello,² M. Werner,⁵³ B. L. Winer,⁵⁹ K. S. Wood,⁶⁰ M. Wood,^{2, ‡} G. Zaharijas,^{61, 62} and S. Zimmer^{3, 4}

(The Fermi-LAT Collaboration)

Fermi dark matter search with Dsphs

- ❖ Case study.
- ❖ The 2015 paper
- ❖ 1. Theory
- ❖ 2. Density profile
- ❖ 3. J-factor

$$\phi_s(\Delta\Omega) = \underbrace{\frac{1}{4\pi} \frac{\langle\sigma v\rangle}{2m_{\text{DM}}^2} \int_{E_{\text{min}}}^{E_{\text{max}}} \frac{dN_\gamma}{dE_\gamma} dE_\gamma}_{\text{particle physics}} \times \underbrace{\int_{\Delta\Omega} \int_{\text{l.o.s.}} \rho_{\text{DM}}^2(\mathbf{r}) dl d\Omega'}_{\text{J-factor}}. \quad (1)$$

J-FACTORS FOR DWARF SPHEROIDAL GALAXIES

The DM content of dSphs can be determined through dynamical modeling of their stellar density and velocity dispersion profiles [23–25]. Recent studies have shown that an accurate estimate of the dynamical mass of a dSph can be derived from measurements of the average stellar velocity dispersion and half-light radius alone [26, 27]. The total mass within the half-light radius and the integrated J-factor have been found to be fairly insensitive to the assumed DM density profile [13, 25, 28]. We assume that the DM distribution in dSphs follows a Navarro-Frenk-White (NFW) profile [29],

$$\rho_{\text{DM}}(r) = \frac{\rho_0 r_s^3}{r(r_s + r)^2}, \quad (2)$$

where r_s and ρ_0 are the NFW scale radius and characteristic density, respectively. We take J-factors and other physical properties for the Milky Way dSphs from Ackermann *et al.* [13] (and references therein).

15 of the observed dSphs⁵ and include statistical uncertainties on the J-factors of each dSph by adding an additional J-factor likelihood term to the binned Poisson likelihood for the LAT data. The J-factor likelihood for target i is given by

$$\mathcal{L}_J(J_i | J_{\text{obs},i}, \sigma_i) = \frac{1}{\ln(10) J_{\text{obs},i} \sqrt{2\pi\sigma_i}} \times e^{-(\log_{10}(J_i) - \log_{10}(J_{\text{obs},i}))^2 / 2\sigma_i^2}, \quad (3)$$

where J_i is the true value of the J-factor and $J_{\text{obs},i}$ is the measured J-factor with error σ_i . This parameterization of the J-factor likelihood is obtained by fitting a log-normal function with peak value $J_{\text{obs},i}$ to the posterior distribution for each J-factor as derived by Martinez [8], providing a reasonable way to quantify the uncertainties on the J-factors. This approach is a slight modification of the approach in Ackermann *et al.* [10, 13], where an effective likelihood was derived considering a flat prior on the J-factors. We note that the J-factor correction is only intended to incorporate the *statistical* uncertainty in the J-factors, and not the systematic uncertainty resulting from the fitting procedure or choice of priors [22]. More details on the derivation of the J-factor likelihood and the effects of systematic uncertainties can be found in Supplemental Material [22].

Dwarf J-factors

- ❖ J-factors from dwarfs can be inferred from the stellar kinematic data

TABLE I. Properties of Milky Way dSphs.

Name	ℓ^a (deg)	b^a (deg)	Distance (kpc)	$\log_{10}(J_{\text{obs}})^b$ ($\log_{10}[\text{GeV}^2 \text{ cm}^{-5}]$)	Ref.
Bootes I	358.1	69.6	66	18.8 ± 0.22	[41]
Canes Venatici II	113.6	82.7	160	17.9 ± 0.25	[42]
Carina	260.1	-22.2	105	18.1 ± 0.23	[43]
Coma Berenices	241.9	83.6	44	19.0 ± 0.25	[42]
Draco	86.4	34.7	76	18.8 ± 0.16	[44]
Fornax	237.1	-65.7	147	18.2 ± 0.21	[43]
Hercules	28.7	36.9	132	18.1 ± 0.25	[42]
Leo II	220.2	67.2	233	17.6 ± 0.18	[45]
Leo IV	265.4	56.5	154	17.9 ± 0.28	[42]
Sculptor	287.5	-83.2	86	18.6 ± 0.18	[43]
Segue 1	220.5	50.4	23	19.5 ± 0.29	[46]
Sextans	243.5	42.3	86	18.4 ± 0.27	[43]
Ursa Major II	152.5	37.4	32	19.3 ± 0.28	[42]
Ursa Minor	105.0	44.8	76	18.8 ± 0.19	[44]
Willman 1	158.6	56.8	38	19.1 ± 0.31	[47]
Bootes II ^c	353.7	68.9	42	—	—
Bootes III	35.4	75.4	47	—	—
Canes Venatici I	74.3	79.8	218	17.7 ± 0.26	[42]
Canis Major	240.0	-8.0	7	—	—
Leo I	226.0	49.1	254	17.7 ± 0.18	[48]
Leo V	261.9	58.5	178	—	—
Pisces II	79.2	-47.1	182	—	—
Sagittarius	5.6	-14.2	26	—	—
Segue 2	149.4	-38.1	35	—	—
Ursa Major I	159.4	54.4	97	18.3 ± 0.24	[42]

^a Galactic longitude and latitude.

^b J-factors are calculated assuming an NFW density profile and integrated over a circular region with a solid angle of $\Delta\Omega \sim 2.4 \times 10^{-4} \text{ sr}$ (angular radius of 0.5°).

^c dSphs below the horizontal line are not included in the combined analysis.

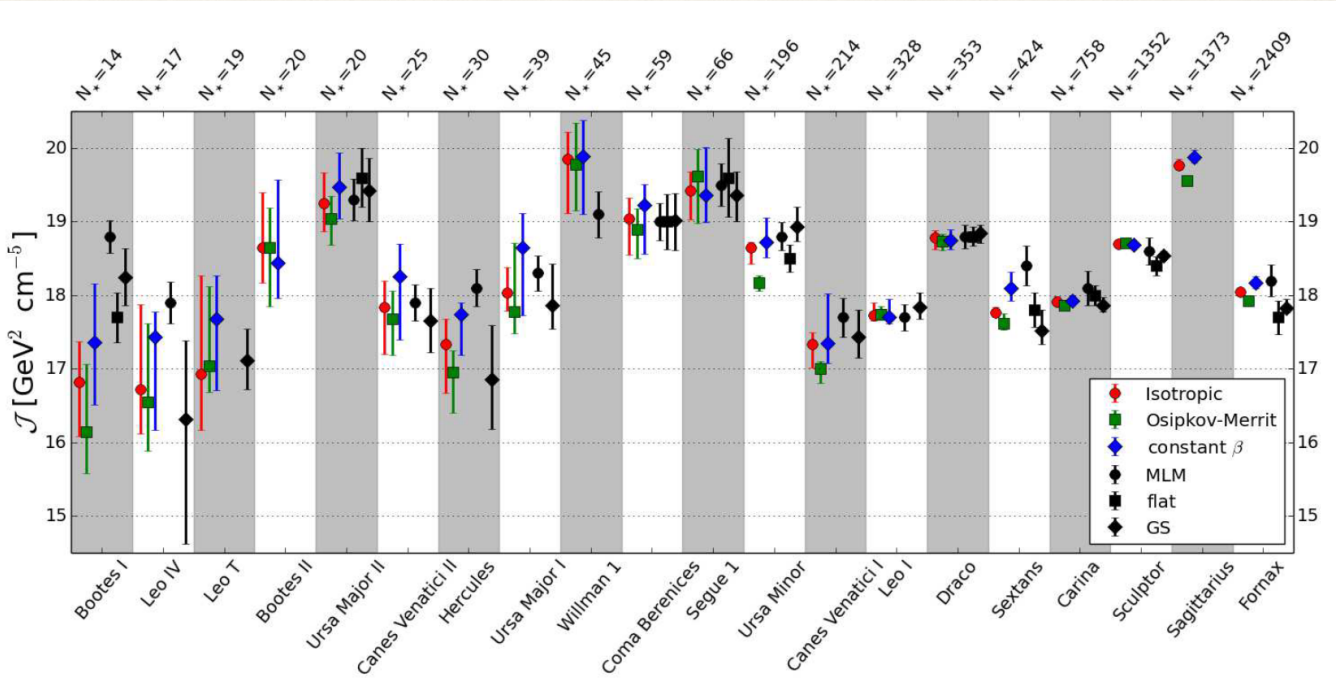
Fermi 2015

term, the *J-factor*, is the line-of-sight (l.o.s.) integral of the DM halo density ρ_{DM} squared (in the case of annihilation), integrated over a solid angle $\Delta\Omega = 2\pi(1 - \cos\theta_{\text{max}})$. It is given by

$$J(D, \Delta\Omega) = \int_{\Delta\Omega} \int_{\text{l.o.s.}} \rho_{\text{DM}}^2(r(s)) ds d\Delta\Omega'. \quad (2)$$

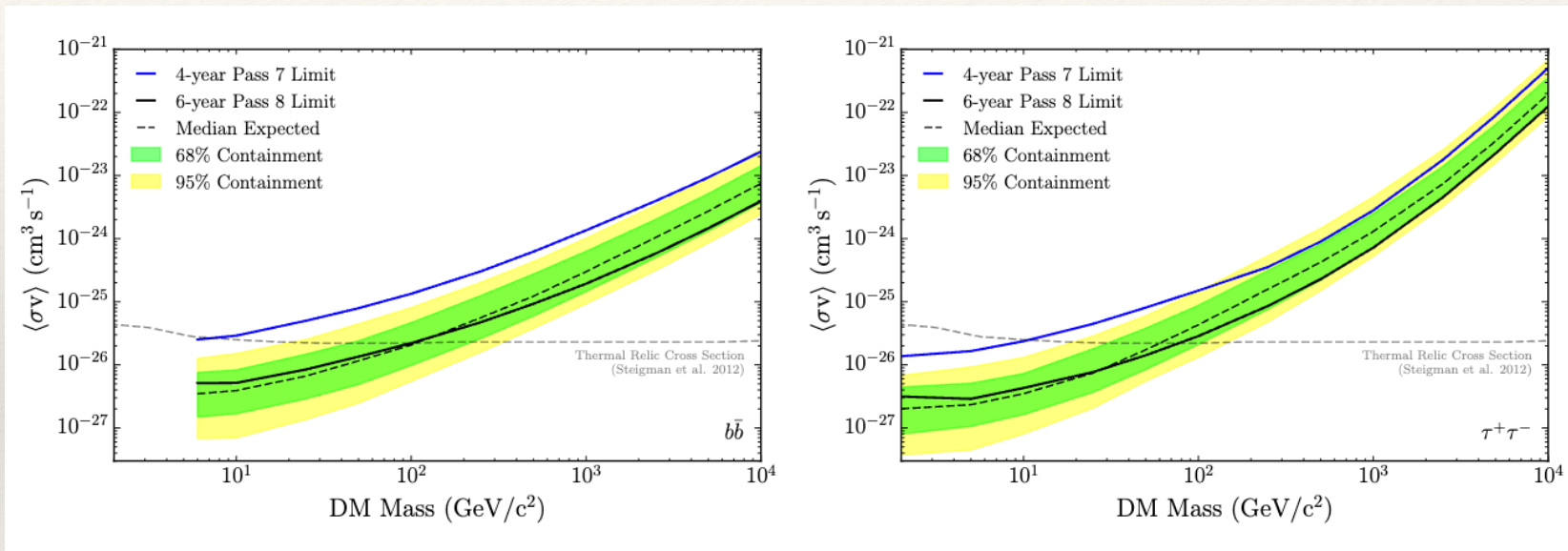
Because of this square density dependence of the flux, regions of density enhancements are targets for DM searches. For instance, $J \approx 10^{22}\text{-}10^{23} \text{ GeV}^2 \text{ cm}^{-5}$ for the Galactic centre (GC), $10^{17}\text{-}10^{19} \text{ GeV}^2 \text{ cm}^{-5}$ for dwarf galaxies, and $10^{15}\text{-}10^{19} \text{ GeV}^2 \text{ cm}^{-5}$ for galaxy clusters (see Conrad et al. 2015 and Charles et al. 2016 for a discussion of different targets for DM searches). These values would place the GC

<https://arxiv.org/pdf/1608.07111.pdf#page=7.68>



Back to Fermi

- ❖ No dark matter were found by performing a statistical test
 - ❖ Null hypothesis
 - ❖ Dark matter hypothesis
- ❖ No significant preference of dark matter in the data
- ❖ For each dark matter mass, for each channel, **obtain an upper limit for the annihilation cross section**



Galactic Center Excess

- ❖ First report in 2009
- ❖ The Galactic is brightest in the Galactic Center
- ❖ If density profile is NFW

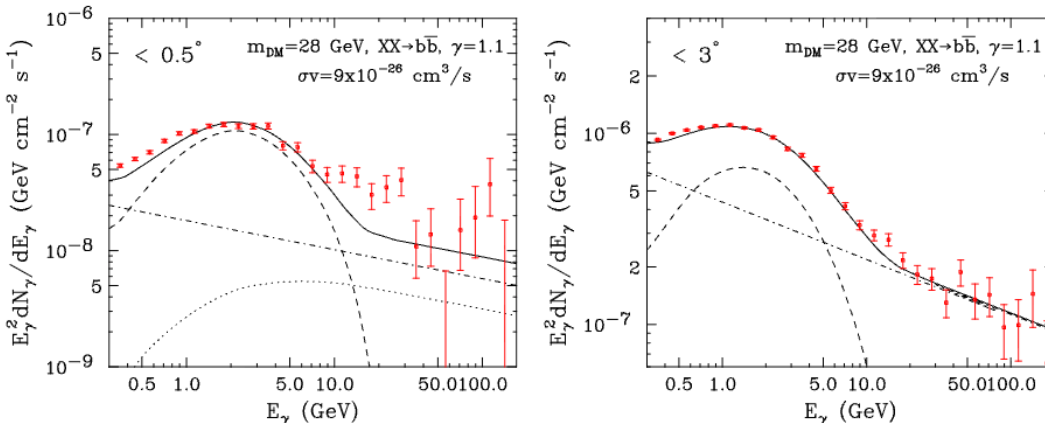
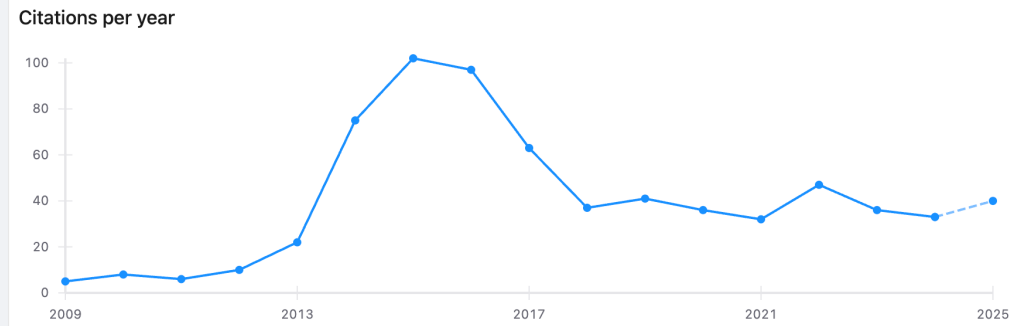


FIG. 2: The gamma ray spectrum measured by the FGST within 0.5° (left) and 3° (right) of the Milky Way's dynamical center. In each frame, the dashed line denotes the predicted spectrum from a 28 GeV dark matter particle annihilating to $b\bar{b}$ with a cross section of $\sigma v = 9 \times 10^{-26} \text{ cm}^3/\text{s}$, and distributed according to a halo profile slightly more cusped than NFW ($\gamma = 1.1$). The dotted and dot-dashed lines denote the contributions from the previously discovered TeV point source located at the Milky Way's dynamical center and the diffuse background, respectively. The solid line is the sum of these contributions.



Possible Evidence For Dark Matter Annihilation In The Inner Milky Way From The Fermi Gamma Ray Space Telescope

Lisa Goodenough, Dan Hooper

We study the gamma rays observed by the Fermi Gamma Ray Space Telescope from the direction of the Galactic Center and find that their angular distribution and energy spectrum are well described by a dark matter annihilation scenario. In particular, we find a good fit to the data for dark matter particles with a $25\text{--}30 \text{ GeV}$ mass, an annihilation cross section of $\sim 9 \times 10^{-26} \text{ cm}^3/\text{s}$, and that are distributed with a cusped halo profile within the inner kiloparsec of the Galaxy. We cannot, however, exclude the possibility that these photons originate from an astrophysical source or sources with a similar morphology and spectral shape to those predicted in an annihilating dark matter scenario.

Comments: 5 pages, 2 figures

Subjects: High Energy Physics – Phenomenology (hep-ph)

Report number: FERMILAB-PUB-09-494-A

Cite as: arXiv:0910.2998 [hep-ph]

(or arXiv:0910.2998v2 [hep-ph] for this version)

<https://doi.org/10.48550/arXiv.0910.2998>

Galactic Center Excess

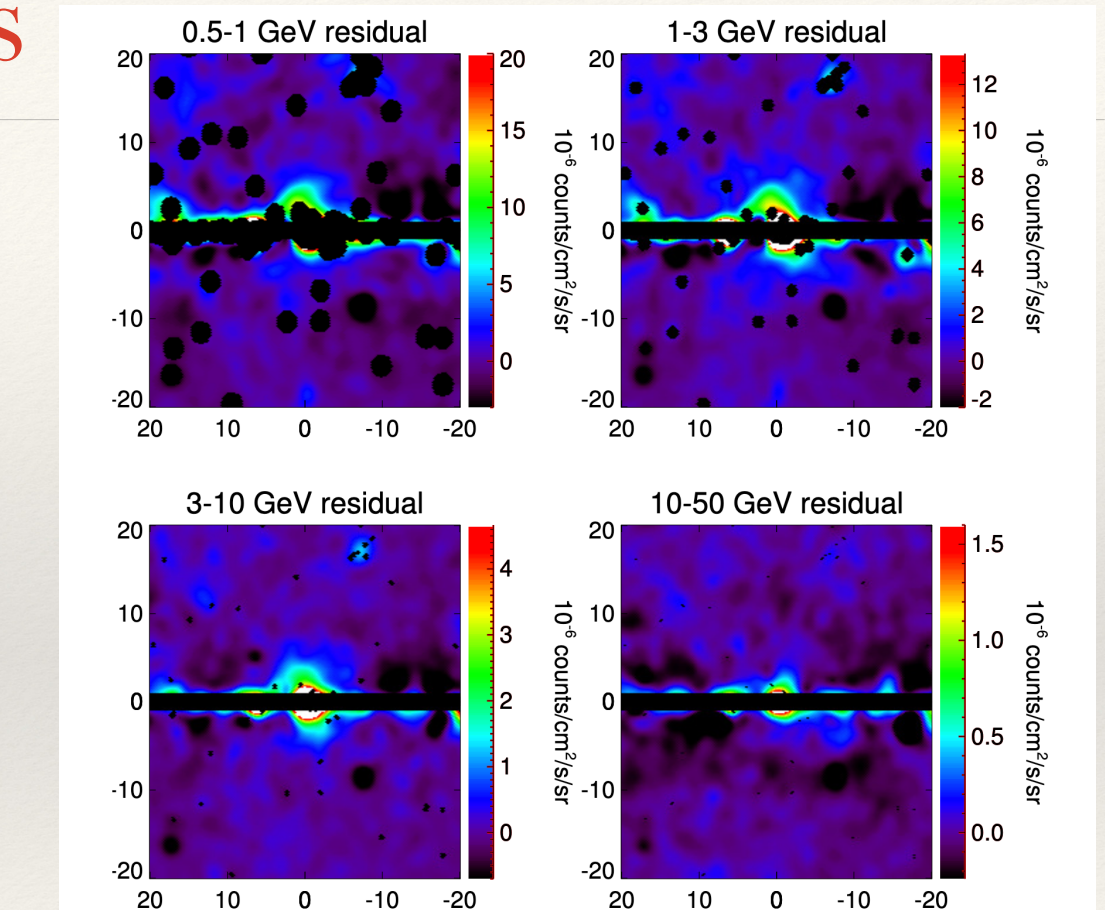
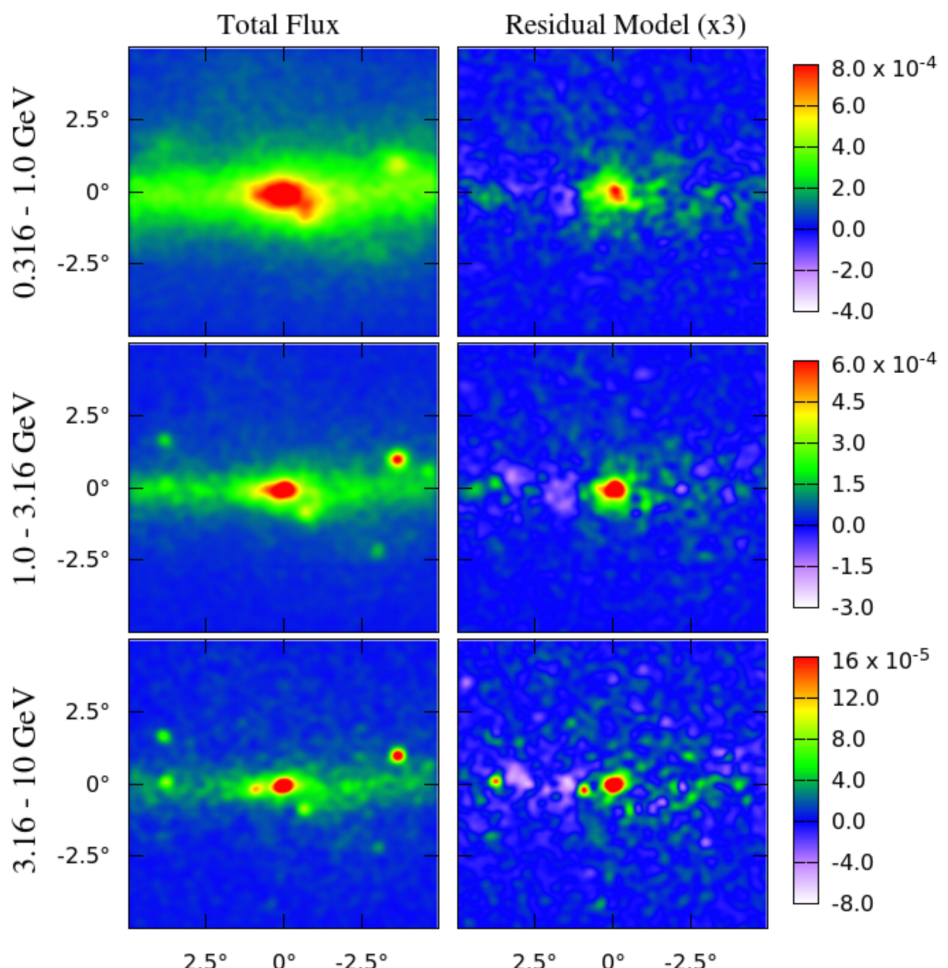


FIG. 7: Intensity maps (in galactic coordinates) after subtracting the point source model and best-fit Galactic diffuse model, *Fermi* bubbles, and isotropic templates. Template coefficients are obtained from the fit including these three templates and a $\gamma = 1.3$ DM-like template. Masked pixels are indicated in black. All maps have been smoothed to a common PSF of 2 degrees for display, before masking (the corresponding masks have *not* been smoothed; they reflect the actual masks used in the analysis). At energies between ~ 0.5 - 10 GeV (*i.e.* in the first three frames), the dark-matter-like emission is clearly visible around the Galactic Center.

GCE

- ❖ Model away the
- ❖ Inverse Compton Emission
- ❖ Pion decay (hadronic)
- ❖ Bremsstrahlung emission

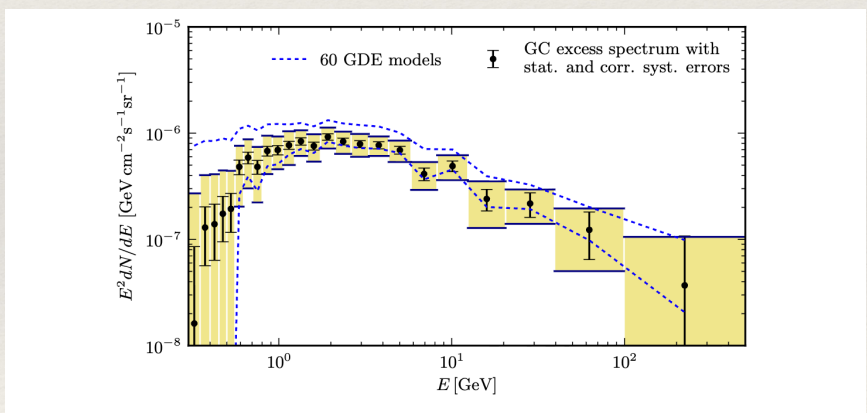
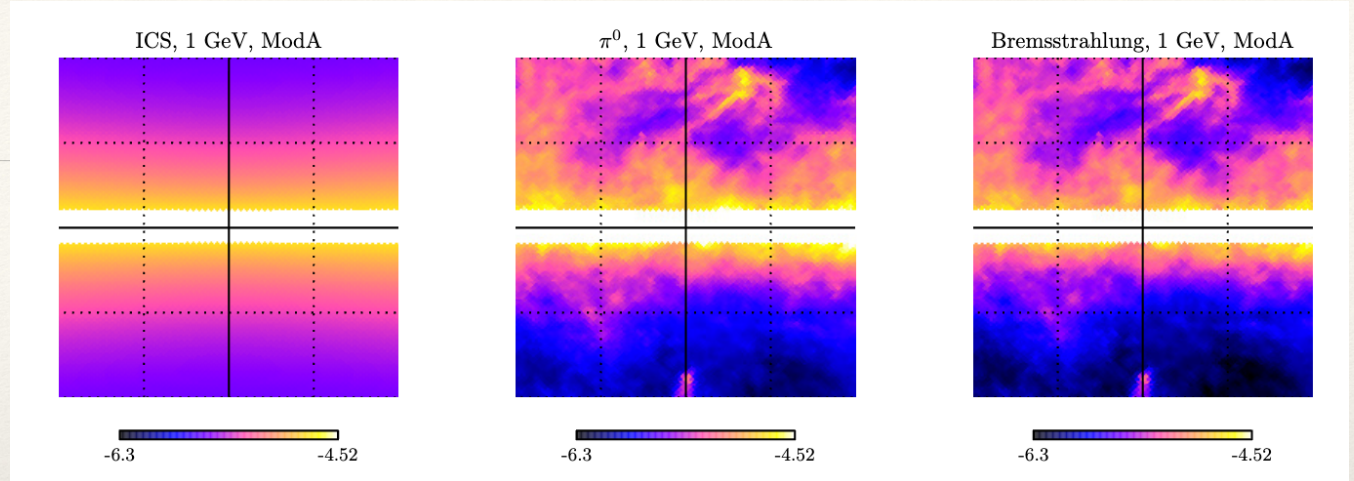


Figure 14. Spectrum of the GCE emission for model F (black dots) together with statistical and systematical (yellow boxes, cf. figure 12) errors. We also show the envelope of the GCE spectrum for all 60 GDE models (blue dashed line, cf. figure 7).

GCE

- ❖ Model away the
- ❖ Inverse Compton Emission
- ❖ Pion decay (hadronic)
- ❖ Bremsstrahlung emission

[https://arxiv.org/pdf/1409.0042](https://arxiv.org/pdf/1409.0042.pdf)

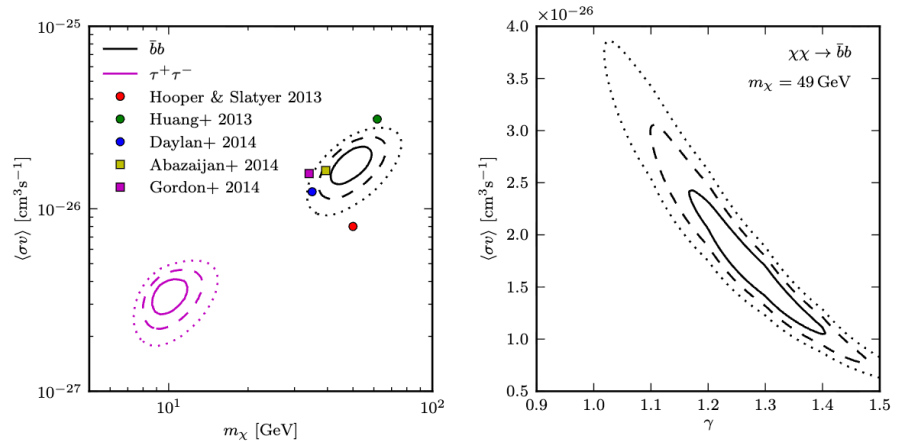


Figure 18. *Left panel:* Constraints on the $\langle\sigma v\rangle$ -vs- m_χ plane for three different DM annihilation channels, from a fit to the spectrum shown in figure 14 (cf. table 4). *Colored points (squares)* refer to best-fit values from previous Inner Galaxy (Galactic center) analyses (see discussion in section 6.2). *Right panel:* Constraints on the $\langle\sigma v\rangle$ -vs- γ plane, based on the fits with the ten GCE segments.

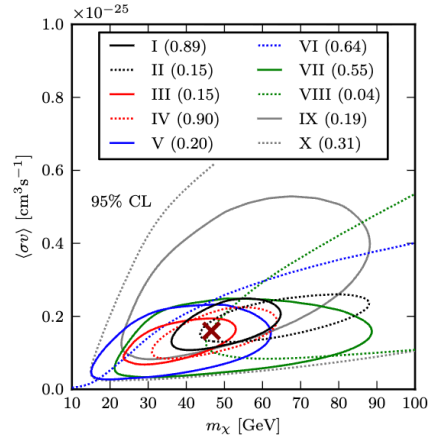


Figure 19. Constraints on the $\langle\sigma v\rangle$ -vs- m_χ plane at 95% CL, individually for the GCE template segments shown in figure 15, for the channel $\chi\chi \rightarrow \bar{b}b$. The cross indicates the best-fit value from a fit to all regions simultaneously ($m_\chi \simeq 46.6$ GeV, $\langle\sigma v\rangle \simeq 1.60 \times 10^{-26}$ $cm^3 s^{-1}$). Note that we assume a NFW profile with an inner slope of $\gamma = 1.28$. The individual p -values are shown in the figure legend; the combined p -value is 0.11.

Astrophysical?

- ❖ Astrophysical emissions
- ❖ Millisecond Pulsars
- ❖ Pulsars spin up by companion stars



FREE ARTICLE

Millisecond Pulsar Origin of the Galactic Center Excess and Extended Gamma-Ray Emission from Andromeda: A Closer Look

Christopher Eckner, Xian Hou, Pasquale D. Serpico, Miles Winter, Gabrijela Zaharijas, Pierrick Martin, Mattia di Mauro, Nestor Mirabal, Jovana Petrovic, Tijana Prodanovic

[▼ Show full author list](#)

Published 2018 July 25 • © 2018. The American Astronomical Society. All rights reserved.

A New Determination of the Millisecond Pulsar Gamma-Ray Luminosity Function and Implications for the Galactic Center Gamma-Ray Excess

Ian Holst, Dan Hooper

It has been suggested that the Galactic Center Gamma-Ray Excess (GCE) could be produced by a large number of centrally-located millisecond pulsars. The fact that no such pulsar population has been detected implies that these sources must be very faint and very numerous. In this study, we use the contents of Fermi's recently released Third Pulsar Catalog (3PC) to measure the luminosity function of the millisecond pulsars in the Milky Way's Disk. We find that this source population exhibits a luminosity function with a mean gamma-ray luminosity of $\langle L_\gamma \rangle \sim 6 \times 10^{32}$ erg/s (integrated above 0.1 GeV). If the GCE were generated by millisecond pulsars with the same luminosity function, we find that ~ 20 such sources from the Inner Galaxy population should have already been detected by Fermi and included in the 3PC. Given the lack of such observed sources, we exclude the hypothesis that the GCE is generated by pulsars with the same luminosity function as those in the Galactic Disk with a significance of 3.4σ . We conclude that either less than 39% of the GCE is generated by pulsars, or that the millisecond pulsars in the Inner Galaxy are at least 5 times less luminous on average than those found in the Galactic Disk.

Abstract

A new measurement of a spatially extended gamma-ray signal from the center of the Andromeda galaxy (M31) has recently been published by the *Fermi*-LAT collaboration, reporting that the emission broadly resembles the so-called Galactic center excess (GCE) of the Milky Way (MW). The weight of the evidence is steadily accumulating on a millisecond pulsar (MSPs) origin for the GCE. These elements prompt us to compare these observations with what is, perhaps, the simplest model for an MSP population, which is solely obtained by rescaling of the MSP luminosity function that is determined in the local MW disk via the respective stellar mass of the systems. Remarkably, we find that without free fitting parameters, this model can account for both the energetics and the morphology of the GCE within uncertainties. For M31, the estimated luminosity due to primordial MSPs is expected to only contribute about a quarter of the detected emission, although a stronger contribution cannot be excluded given the large uncertainties. If correct, the model predicts that the M31 disk emission due to MSPs is not far below the present upper bound. We also discuss additional refinements of this simple model. Using the correlation between globular cluster gamma-ray luminosity and stellar encounter rate, we gauge the dynamical MSP formation in the bulge. This component is expected to contribute to the GCE only at a level of $\leq 5\%$, it could affect the signal's morphology. We also comment on the limitations of our model and on future perspectives for improved diagnostics.

Help from new techniques

Dark Matter Strikes Back at the Galactic Center

Rebecca K. Leane, Tracy R. Slatyer

Statistical evidence has previously suggested that the Galactic Center GeV Excess (GCE) originates largely from point sources, and not from annihilating dark matter. We examine the impact of unmodeled source populations on identifying the true origin of the GCE using non-Poissonian template fitting (NPTF) methods. In a proof-of-principle example with simulated data, we discover that unmodeled sources in the Fermi Bubbles can lead to a dark matter signal being misattributed to point sources by the NPTF. We discover striking behavior consistent with a mismodeling effect in the real Fermi data, finding that large artificial injected dark matter signals are completely misattributed to point sources. Consequently, we conclude that dark matter may provide a dominant contribution to the GCE after all.

Distinguishing Dark Matter from Unresolved Point Sources in the Inner Galaxy with Photon Statistics

Samuel K. Lee, Mariangela Lisanti, Benjamin R. Safdi

Data from the Fermi Large Area Telescope suggests that there is an extended excess of GeV gamma-ray photons in the Inner Galaxy. Identifying potential astrophysical sources that contribute to this excess is an important step in verifying whether the signal originates from annihilating dark matter. In this paper, we focus on the potential contribution of unresolved point sources, such as millisecond pulsars (MSPs). We propose that the statistics of the photons---in particular, the flux probability density function (PDF) of the photon counts below the point-source detection threshold---can potentially distinguish between the dark-matter and point-source interpretations. We calculate the flux PDF via the method of generating functions for these two models of the excess. Working in the framework of Bayesian model comparison, we then demonstrate that the flux PDF can potentially provide evidence for an unresolved MSP-like point-source population.

Evidence for Unresolved Gamma-Ray Point Sources in the Inner Galaxy

Samuel K. Lee, Mariangela Lisanti, Benjamin R. Safdi, Tracy R. Slatyer, Xue

We present a new method to characterize unresolved point sources (PSs), generalizing traditional template fits to account for non-Poissonian photon statistics. We apply this method to Fermi Large Area Telescope gamma-ray data to characterize PS populations at high latitudes and in the Inner Galaxy. We find that PSs (resolved and unresolved) account for ~50% of the total extragalactic gamma-ray background in the energy range ~1.9 to 11.9 GeV. Within 10° of the Galactic Center with $|b| \geq 2^\circ$, we find that ~5–10% of the flux can be accounted for by a population of unresolved PSs, distributed consistently with the observed ~GeV gamma-ray excess in this region. The excess is fully absorbed by such a population, in preference to dark-matter annihilation. The inferred source population is dominated by near-threshold sources, which may be detectable in future searches.

GCE

- ❖ Currently the most intriguing dark matter “signal”
- ❖ If DM hypothesis is true, must need to be seen in other dark matter sources
 - ❖ None have so far in DSph analysis, etc.
- ❖ Too bad Fermi itself probably cannot resolve this issue.
 - ❖ 16 years of data already

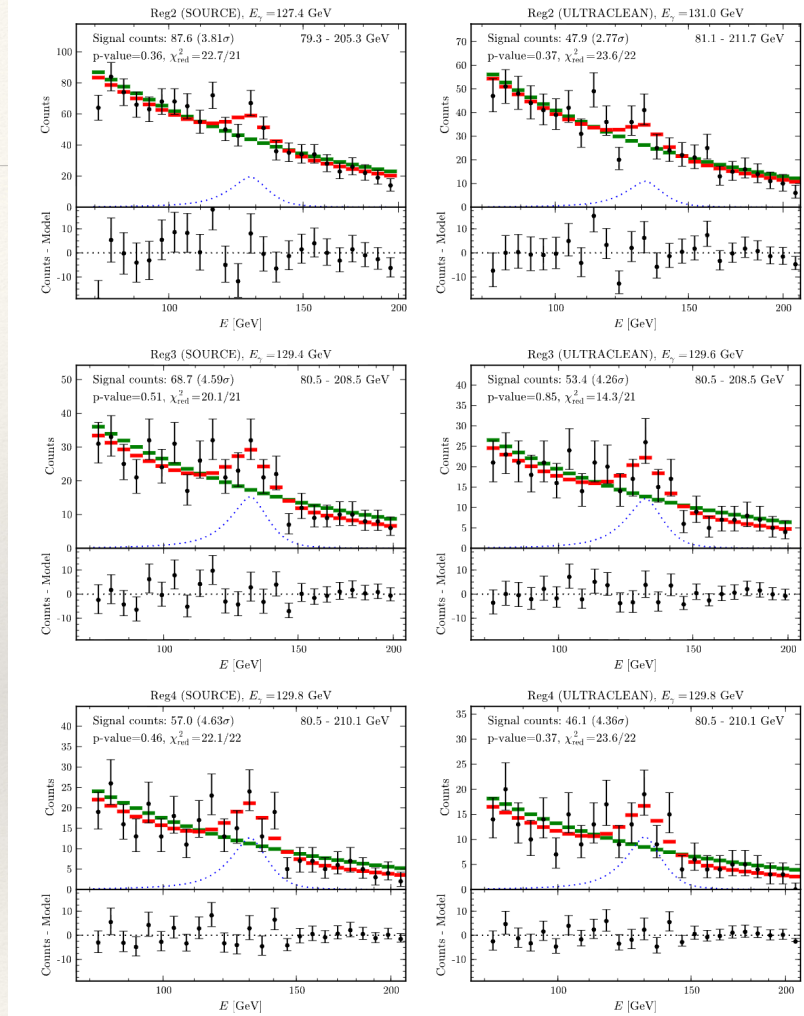
130 GeV line

- ❖ If a continuum signal can be confused with astrophysical sources, lets look for smoking guns
- ❖ Dark Matter annihilating to photons
- ❖ A spectral line with no astrophysical counterpart in gamma rays

A Tentative Gamma-Ray Line from Dark Matter Annihilation at the Fermi Large Area Telescope

Christoph Weniger

The observation of a gamma-ray line in the cosmic-ray fluxes would be a smoking-gun signature for dark matter annihilation or decay in the Universe. We present an improved search for such signatures in the data of the Fermi Large Area Telescope (LAT), concentrating on energies between 20 and 300 GeV. Besides updating to 43 months of data, we use a new data-driven technique to select optimized target regions depending on the profile of the Galactic dark matter halo. In regions close to the Galactic center, we find a 4.6 sigma indication for a gamma-ray line at 130 GeV. When taking into account the look-elsewhere effect the significance of the observed excess is 3.2 sigma. If interpreted in terms of dark matter particles annihilating into a photon pair, the observations imply a dark matter mass of $129.8 \pm 2.4^{+7}_{-13}$ GeV and a partial annihilation cross-section of $\langle \sigma v \rangle = 1.27 \pm 0.32^{+0.18}_{-0.28} \times 10^{-27} \text{ cm}^3 \text{ s}^{-1}$ when using the Einasto dark matter profile. The evidence for the signal is based on about 50 photons; it will take a few years of additional data to clarify its existence.



Too bad it looks like a systematic detector issue

- ❖ Dark Matter searches are always pushing the limits of detectors
- ❖ By definition the signal is weak

Search for Gamma-ray Spectral Lines with the Fermi Large Area Telescope and Dark Matter Implications

Fermi-LAT Collaboration

Weakly Interacting Massive Particles (WIMPs) are a theoretical class of particles that are excellent dark matter candidates. WIMP annihilation or decay may produce essentially monochromatic gamma rays detectable by the Fermi Large Area Telescope (LAT) against the astrophysical gamma-ray emission of the Galaxy. We have searched for spectral lines in the energy range 5–300 GeV using 3.7 years of data, reprocessed with updated instrument calibrations and an improved energy dispersion model compared to the previous Fermi-LAT Collaboration line searches. We searched in five regions selected to optimize sensitivity to different theoretically-motivated dark matter density distributions. We did not find any globally significant lines in our a priori search regions and present 95% confidence limits for annihilation cross sections of self-conjugate WIMPs and decay lifetimes. Our most significant fit occurred at 133 GeV in our smallest search region and had a local significance of 3.3 standard deviations, which translates to a global significance of 1.5 standard deviations. We discuss potential systematic effects in this search, and examine the feature at 133 GeV in detail. We find that both the use of reprocessed data and of additional information in the energy dispersion model contribute to the reduction in significance of the line-like feature near 130 GeV relative to significances reported in other works. We also find that the feature is narrower than the LAT energy resolution at the level of 2 to 3 standard deviations, which somewhat disfavors the interpretation of the 133 GeV feature as a real WIMP signal.

2025 story

arXiv > astro-ph > arXiv:2507.07209

Search..
Help | Ad

Astrophysics > High Energy Astrophysical Phenomena

[Submitted on 9 Jul 2025 (v1), last revised 23 Nov 2025 (this version, v3)]

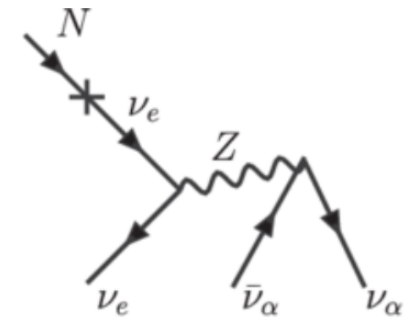
20 GeV halo-like excess of the Galactic diffuse emission and implications for dark matter annihilation

Tomonori Totani

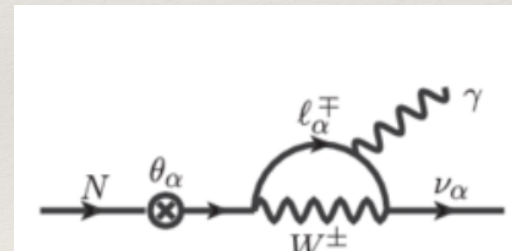
Fifteen years of the Fermi Large Area Telescope (LAT) data in the halo region of the Milky Way (MW) are analyzed to search for gamma rays from dark matter annihilation. Gamma-ray maps within the region of interest ($|l| \leq 60^\circ$, $10^\circ \leq |b| \leq 60^\circ$) are modeled using point sources, the GALPROP models of cosmic-ray interactions, isotropic background, and templates of Loop I and the Fermi bubbles, and then the presence of a halo-like component is further examined. A statistically significant halo-like excess is found with a spectral peak around 20 GeV, while its flux is consistent with zero below 2 GeV and above 200 GeV. Examination of the fit residual maps indicates that a spherically symmetric halo component fits the map data well. The radial profile agrees with annihilation by the smooth NFW density profile, and may be slightly shallower than this, especially in the central region. Various systematic uncertainties are investigated, but the 20 GeV peak remains significant. In particular, the halo excess with a similar spectrum is detected even relative to the LAT standard background model, which contains non-template patches adjusted to match the observed map. The halo excess spectrum can be fitted by annihilation with a particle mass $m_\chi \sim 0.5\text{--}0.8$ TeV and cross section $\langle\sigma v\rangle \sim (5\text{--}8) \times 10^{-25}$ $\text{cm}^3 \text{s}^{-1}$ for the $b\bar{b}$ channel. This cross section is larger than the upper limits from dwarf galaxies and the canonical thermal relic value, but considering various uncertainties, especially the density profile of the MW halo, the dark matter interpretation of the 20 GeV ``Fermi halo" remains feasible. The prospects for verification through future observations are briefly discussed.

Sterile Neutrino dark matter

- ❖ Sterile Neutrino dark matter can decay due to the small mixing with active neutrinos
- ❖ The primary decay is to 3 active neutrinos
 - ❖ Which is very difficult to decay
 - ❖ No keV neutrinos has been detected
 - ❖ (Can you help find a way?)
- ❖ There is a radiative decay mode
 - ❖ $\nu_s \rightarrow \nu_a + \gamma$
- ❖ It is a two body decay mode
 - ❖ A photon like at half of the dark matter mass!



(a) Decay of sterile neutrino $N \rightarrow \nu_e \nu_\alpha \bar{\nu}_\alpha$ through neutral current interactions. A virtual ν_e is created and the quadratic mixing (marked by symbol “ \times ”) is proportional to θ^2 .



(c) Two-body decay of sterile neutrino. The energy of the photon is $E_\gamma = \frac{1}{2} M_N$.

Dark Matter Decay search

❖ Annihilation

$$\diamond \epsilon \equiv \frac{1}{2} \left(\frac{\rho_\chi}{m_\chi} \right)^2 \sigma v dV \frac{dN}{dE}$$

$$\diamond \frac{dF}{dE} = \frac{\sigma v}{8\pi m_\chi^2} \frac{dN}{dE} \times \int d\ell d\Omega \rho_\chi^2$$

$$\diamond \frac{dF}{dEd\Omega} = \frac{\sigma v}{8\pi m_\chi^2} \frac{dN}{dE} \times \int d\ell \rho_\chi^2$$

❖

❖ Decay

❖ Consider the decay rate $\Gamma = \frac{1}{\tau}$

$$\diamond \epsilon \equiv \left(\frac{\rho_\chi}{m_\chi} \right) \Gamma dV \frac{dN}{dE}$$

$$\diamond \frac{dF}{dE} = \frac{\Gamma}{4\pi m_\chi} \frac{dN}{dE} \times \int d\ell d\Omega \rho_\chi$$

$$\diamond \frac{dF}{dEd\Omega} = \frac{\Gamma}{4\pi m_\chi} \frac{dN}{dE} \times \int d\ell \rho_\chi$$

❖ Decay vs Annihilation

❖ 1 power of density

❖ Less sensitive to high density regions like the galactic centre !!

Case Study: 3.5 keV Line



Astrophysics > Cosmology and Nongalactic Astrophysics

[Submitted on 10 Feb 2014 (v1), last revised 9 Jun 2014 (this version, v2)]

Detection of An Unidentified Emission Line in the Stacked X-ray spectrum of Galaxy Clusters

Esra Bulbul, Maxim Markevitch, Adam Foster, Randall K. Smith, Michael Loewenstein, Scott W. Randall

We detect a weak unidentified emission line at $E=(3.55-3.57)+/-0.03$ keV in a stacked XMM spectrum of 73 galaxy clusters spanning a redshift range 0.01–0.35. MOS and PN observations independently show the presence of the line at consistent energies. When the full sample is divided into three subsamples (Perseus, Centaurus+Ophiuchus+Coma, and all others), the line is significantly detected in all three independent MOS spectra and the PN "all others" spectrum. It is also detected in the Chandra spectra of Perseus with the flux consistent with XMM (though it is not seen in Virgo). However, it is very weak and located within 50–110eV of several known faint lines, and so is subject to significant modeling uncertainties. On the origin of this line, we argue that there should be no atomic transitions in thermal plasma at this energy. An intriguing possibility is the decay of sterile neutrino, a long-sought dark matter particle candidate. Assuming that all dark matter is in sterile neutrinos with $m_s=2E=7.1$ keV, our detection in the full sample corresponds to a neutrino decay mixing angle $\sin^2(2\theta)=7e-11$, below the previous upper limits. However, based on the cluster masses and distances, the line in Perseus is much brighter than expected in this model. This appears to be because of an anomalously bright line at $E=3.62$ keV in Perseus, possibly an Ar XVII dielectronic recombination line, although its flux would be 30 times the expected value and physically difficult to understand. In principle, such an anomaly might explain our line detection in other subsamples as well, though it would stretch the line energy uncertainties. Another alternative is the above anomaly in the Ar line combined with the nearby 3.51 keV K line also exceeding expectation by factor 10–20. Confirmation with Chandra and Suzaku, and eventually Astro-H, are required to determine the nature of this new line.(ABRIDGED)



Astrophysics > Cosmology and Nongalactic Astrophysics

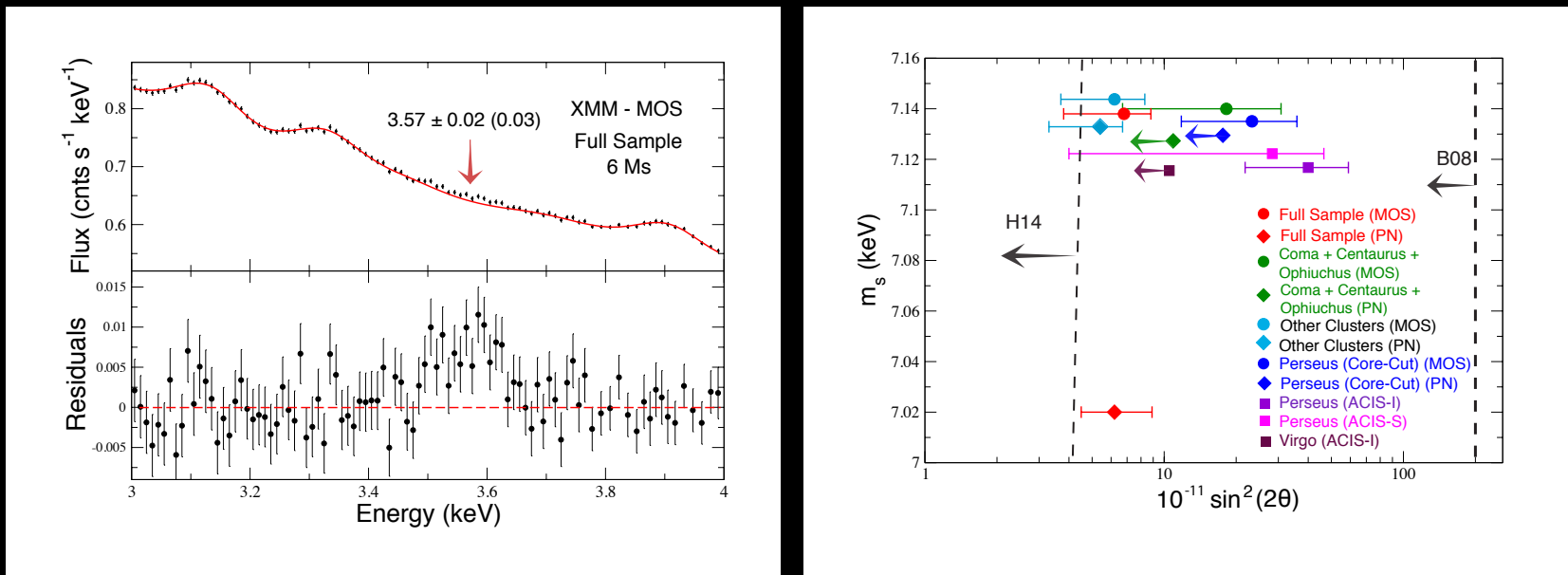
[Submitted on 17 Feb 2014 (v1), last revised 2 Oct 2015 (this version, v2)]

An unidentified line in X-ray spectra of the Andromeda galaxy and Perseus galaxy cluster

Alexey Boyarsky, Oleg Ruchayskiy, Dmytro Iakubovskiy, Jeroen Franse

We report a weak line at $3.52+/-0.02$ keV in X-ray spectra of M31 galaxy and the Perseus galaxy cluster observed by MOS and PN cameras of XMM-Newton telescope. This line is not known as an atomic line in the spectra of galaxies or clusters. It becomes stronger towards the centers of the objects; is stronger for Perseus than for M31; is absent in the spectrum of a deep "blank sky" dataset. Although for each object it is hard to exclude that the feature is due to an instrumental effect or an atomic line, it is consistent with the behavior of a dark matter decay line. Future (non-)detections of this line in multiple objects may help to reveal its nature.

3.5 keV line excess!



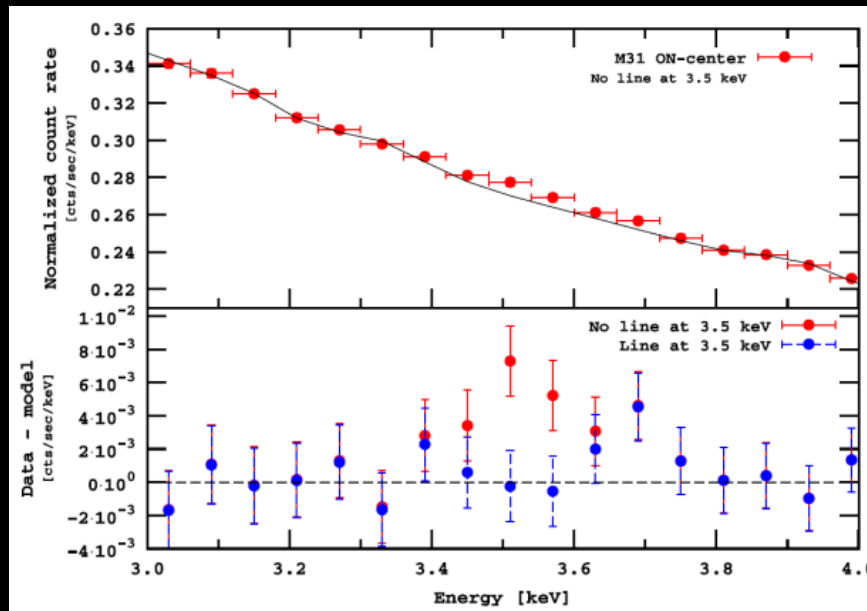
Stacked 73 clusters XMM-MOS (4-5 σ)

Also

Chandra Perseus 2.5 σ and 3.4 σ

3.5 keV line excess!

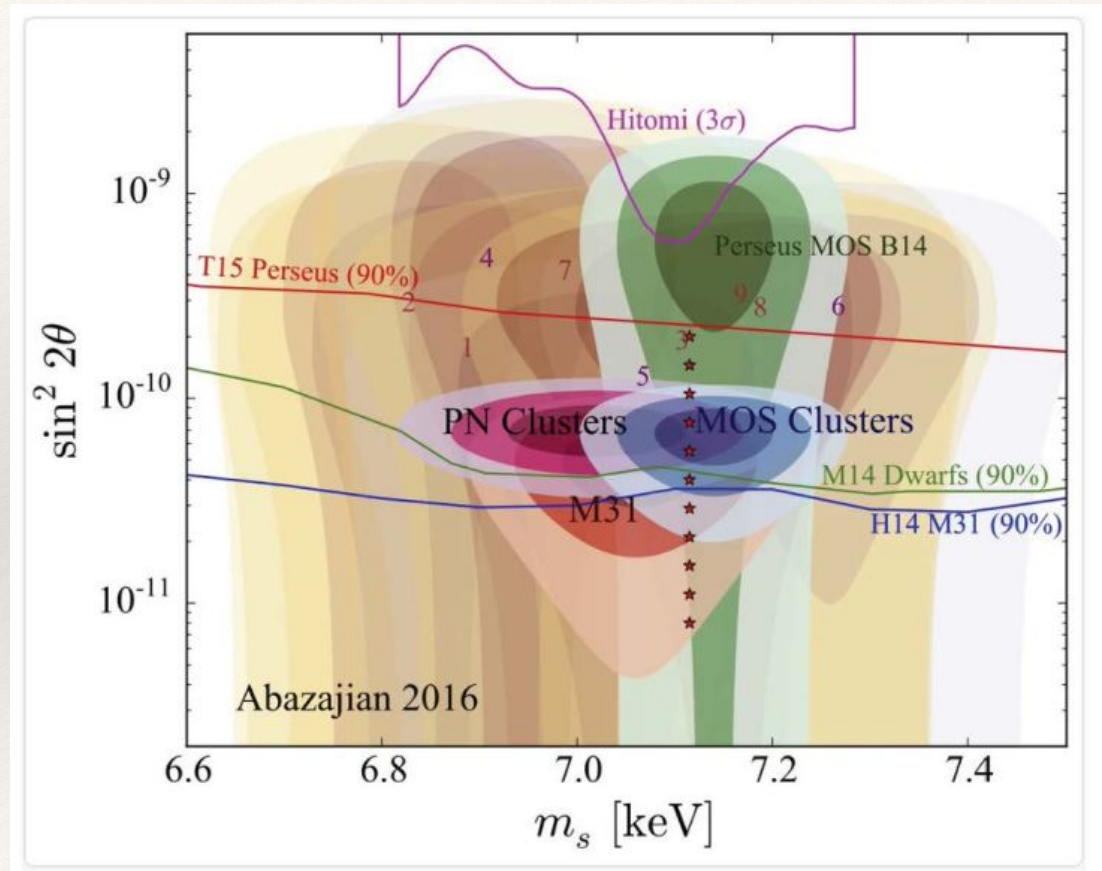
- Boyarsky et al (2014)



$$\sin^2(2\theta) \sim 2-20 \times 10^{-11}$$

Case Study: 3.5 keV Line

- ❖ For a while many papers reported positive detections and many report null detections
- ❖ Challenge
 - ❖ Weak signal
 - ❖ Presence of astrophysical backgrounds
 - ❖ Atomic transitions in X-rays!
- ❖ Luckily
 - ❖ Many x-ray instruments
 - ❖ XMM newton, Chandra, NuSTAR, etc etc



The dark matter interpretation of the 3.5-keV line is inconsistent with blank-sky observations

Christopher Dessert, Nicholas L. Rodd, Benjamin R. Safdi

Observations of nearby galaxies and galaxy clusters have reported an unexpected X-ray emission line around 3.5 kilo-electron volts (keV). Proposals to explain this line include decaying dark matter—in particular, that the decay of sterile neutrinos with a mass around 7 keV could match the available data. If this interpretation is correct, the 3.5 keV line should also be emitted by dark matter in the halo of the Milky Way. We used more than 30 megaseconds of XMM–Newton (X-ray Multi-Mirror Mission) blank-sky observations to test this hypothesis, finding no evidence of the 3.5-keV line emission from the Milky Way halo. We set an upper limit on the decay rate of dark matter in this mass range, which is inconsistent with the possibility that the 3.5-keV line originates from dark matter decay.

arXiv > astro-ph > arXiv:2004.06170

Search...
Help | Advanced

Astrophysics > High Energy Astrophysical Phenomena

[Submitted on 13 Apr 2020]

Technical Comment on "The dark matter interpretation of the 3.5-keV line is inconsistent with blank-sky observations"

Kevork N. Abazajian

I show that model dependencies in the analysis by Dessert, Rodd & Safdi (2020) relax their claimed constraint by a factor of ~20. After including conservative model choices, the derived limits are comparable to or slightly better than limits from previous searches. Further model tests and expansion of the data energy may enhance or relax sensitivity of the methodology.

arXiv > astro-ph > arXiv:2004.06601

Search...
Help | Advanced

Astrophysics > Cosmology and Nongalactic Astrophysics

[Submitted on 14 Apr 2020 (v1), last revised 24 Feb 2021 (this version, v2)]

Response to a comment on Dessert et al. "The dark matter interpretation of the 3.5 keV line is inconsistent with blank-sky observations"

Christopher Dessert, Nicholas L. Rodd, Benjamin R. Safdi

The dark matter explanation of the 3.5 keV line is strongly disfavored by our work in Dessert et al. 2020. Boyarsky et al. 2020 questions that conclusion: modeling additional background lines is claimed to weaken the limit sufficiently to re-allow a dark matter interpretation. We respond as follows. 1) A more conservative limit is obtained by modeling additional lines; this point appeared in its entirety in our work in Dessert et al., though we also showed that the inclusion of such lines is not necessary. 2) Despite suggestions in Boyarsky et al., even the more conservative limits strongly disfavor a decaying dark matter origin of the 3.5 keV line.

3.5 keV line

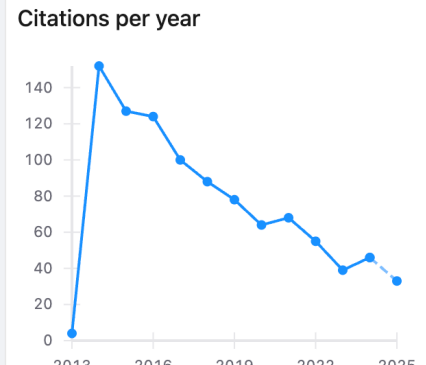
- ❖ My take
- ❖ No Strong independent verifications
- ❖ Especially no such detection with new generation of detectors

Detection of An Unidentified Emission Line in the Stacked X-ray spectrum of Galaxy Clusters

Esra Bulbul (Harvard-Smithsonian Ctr. Astrophys. and NASA, Goddard and CRESST, Greenbelt), Maxim Markevitch (NASA, Goddard), Adam Foster (Harvard-Smithsonian Ctr. Astrophys.), Randall K. Smith (Harvard-Smithsonian Ctr. Astrophys.), Michael Loewenstein (NASA, Goddard and CRESST, Greenbelt and Maryland U.) [Show All\(6\)](#)
Feb 10, 2014

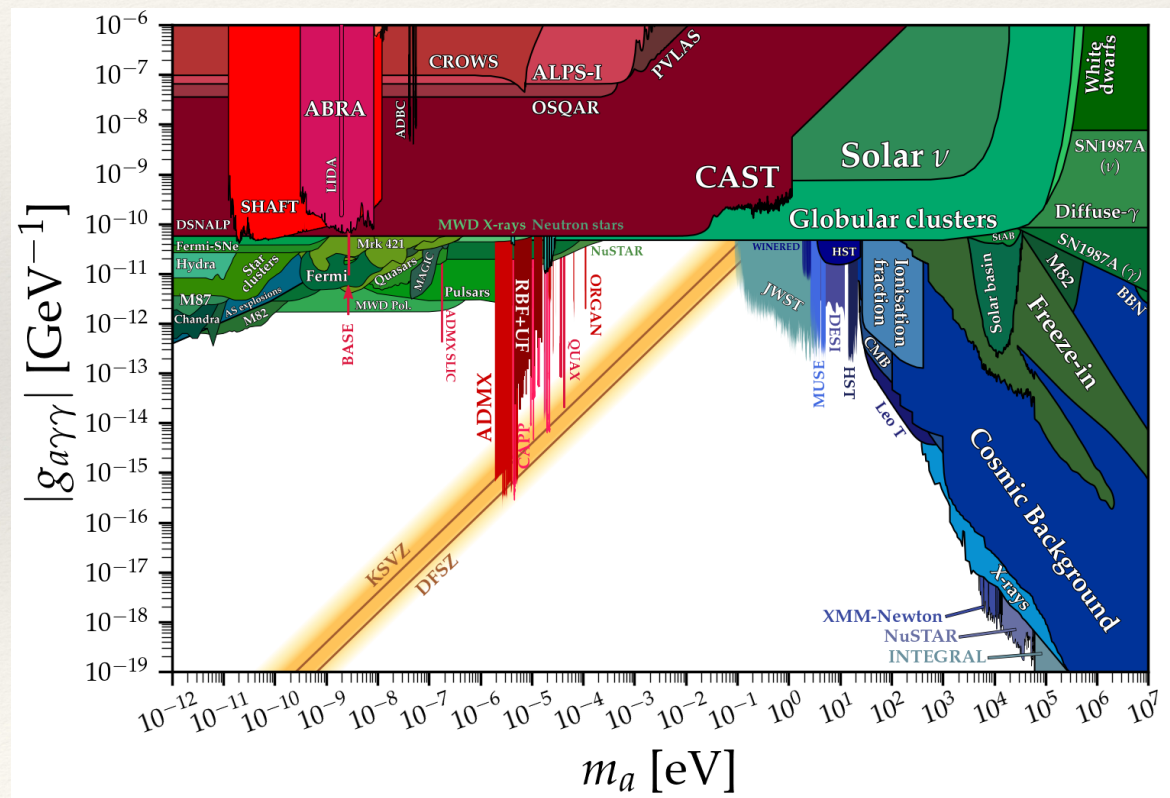
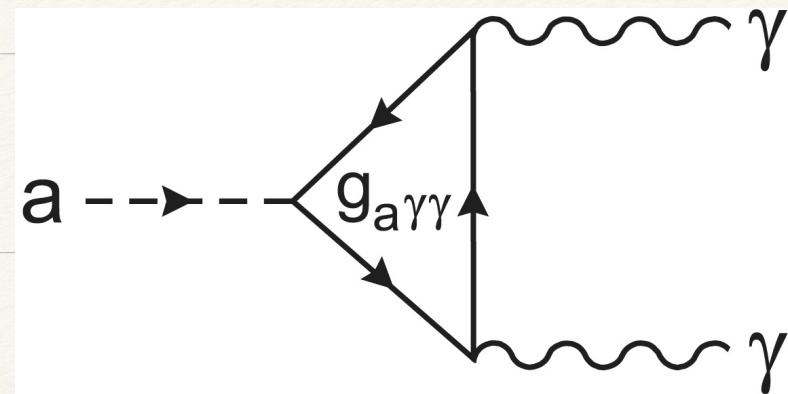
23 pages
Published in: *Astrophys.J.* 789 (2014) 13
Published: 2014
e-Print: [1402.2301](#) [astro-ph.CO]
DOI: [10.1088/0004-637X/789/1/13](#)
View in: [ADS Abstract Service](#)

[pdf](#) [links](#) [cite](#) [claim](#) [reference search](#) [978 citations](#)



Axion dark matter

- ❖ Axions can also decay into two photons
- ❖ In this case, the search is exactly the same as sterile neutrinos
- ❖ The bluish regions comes from photon line searches



PBH dark matter

- ❖ For PBH that are light
 - ❖ (Black holes temperature inverse proportional to its mass)
- ❖ They emit Hawking radiation.
- ❖ In this case their detection is similar to dark matter decays
- ❖ There is still a window that PBH can be 100% dark matter

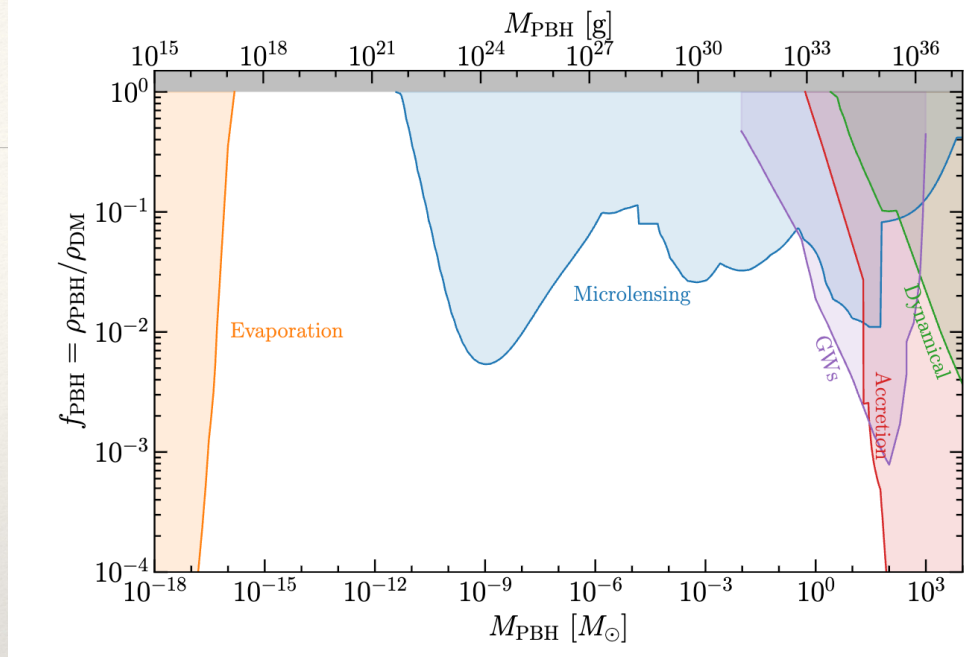


Figure 4: Constraints on the fraction of DM in the form of PBHs, f_{PBHs} , as a function of mass, M_{PBH} , assuming all PBHs have the same mass. The bounds shown are (from left to right) from evaporation (in orange), microlensing (blue), gravitational waves (purple), accretion (red) and dynamical (green). For each type of bound the tightest constraint at each mass is shown and the shaded regions are excluded. Figure created using the PBHbounds code (Kavanagh).

Dark Matter searches of other messengers

- ❖ Electron and positrons
- ❖ We discussed how to model electron positrons
- ❖ Dark Matter annihilating or decaying into electron or positrons can be treated simply by considering the production term.

4.1 Propagation functions

4.1.1 Electrons or positrons: full formalism

The differential e^\pm flux ⁹ per unit of energy from DM annihilations or decays in any point in space \vec{x} and time t is given by $d\Phi_{e^\pm}/dE(t, \vec{x}, E) = v_{e^\pm} f/4\pi$ (units $1/\text{GeV}\cdot\text{cm}^2\cdot\text{s}\cdot\text{sr}$) where v_{e^\pm} is the velocity (essentially equal to c in the regimes of our interest). The e^\pm number density per unit energy, $f(t, \vec{x}, E) = dN_{e^\pm}/dE$, obeys the diffusion-loss equation [100]:

$$\frac{\partial f}{\partial t} - \nabla(\mathcal{K}(E, \vec{x}) \nabla f) - \frac{\partial}{\partial E}(b(E, \vec{x})f) = Q(E, \vec{x}) \quad (7)$$

$\rho(\vec{x})$ provide the source term Q of eq. (7), which reads

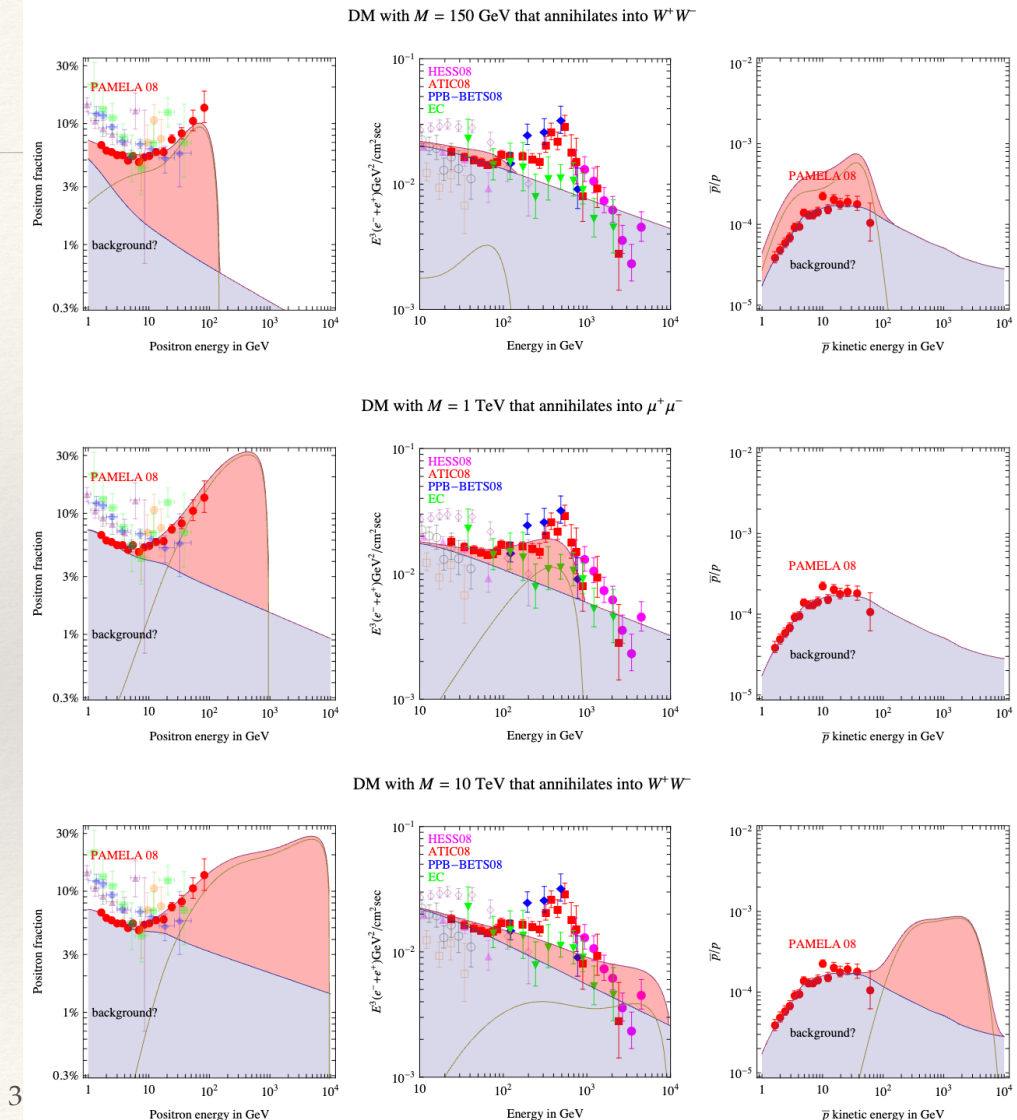
$$Q = \frac{1}{2} \left(\frac{\rho}{M_{\text{DM}}} \right)^2 f_{\text{inj}}^{\text{ann}}, \quad f_{\text{inj}}^{\text{ann}} = \sum_f \langle \sigma v \rangle_f \frac{dN_{e^\pm}^f}{dE} \quad (\text{annihilation}), \quad (11)$$

$$Q = \left(\frac{\rho}{M_{\text{DM}}} \right) f_{\text{inj}}^{\text{dec}}, \quad f_{\text{inj}}^{\text{dec}} = \sum_f \Gamma_f \frac{dN_{e^\pm}^f}{dE} \quad (\text{decay}), \quad (12)$$

where f runs over all the channels with e^\pm in the final state, with the respective thermal averaged cross sections σv or decay rate Γ .

Case study: Positron fraction

- ❖ Electron and positrons
- ❖ We discussed how to model electron positrons
- ❖ Dark Matter annihilating or decaying into electron or positrons can be treated simply by considering the production term.



Case study: Positron fraction

- ❖ Electron and positrons
- ❖ We discussed how to model electron positrons
- ❖ Dark Matter annihilating or decaying into electron or positrons can be treated simply by considering the production term.
- ❖ How can the cross section be so big?

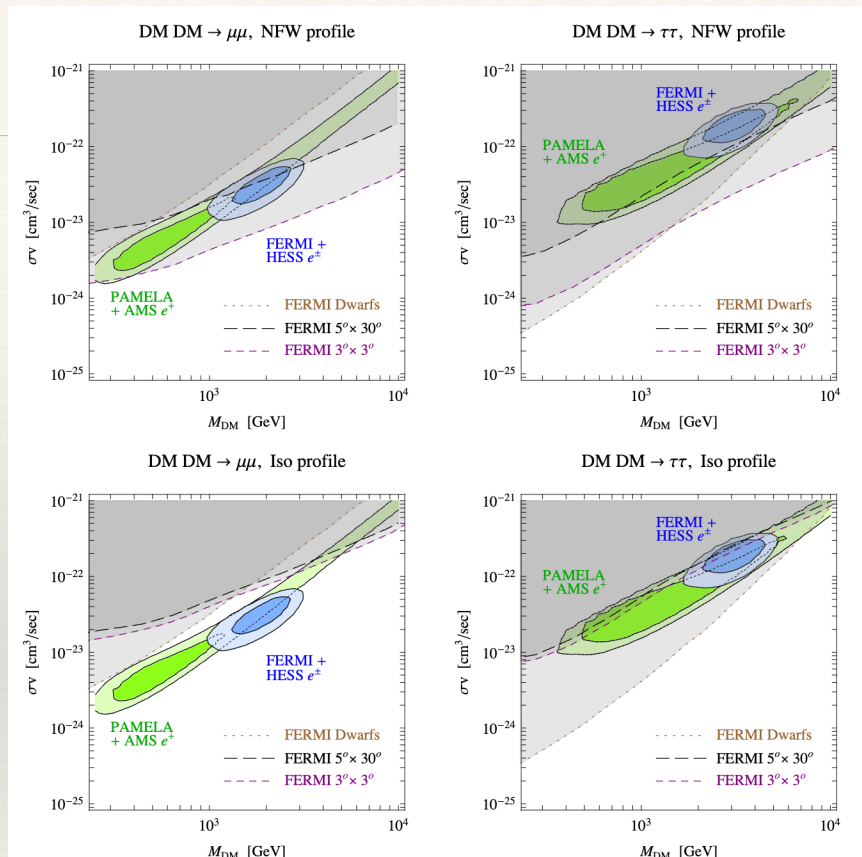


Figure 14: Regions of the $(M, \sigma v)$ plane favoured by AMS and PAMELA measurements of the positron fraction (green) and by FERMI and HESS measurements of the electron and positron fluxes (blue), both at 3σ and 5σ , for the $\mu^+\mu^-$ (left) and $\tau^+\tau^-$ annihilation channel (right), compared to representative γ -ray constraints for the NFW (upper) and isothermal (lower) DM density profiles.

Case study: Positron fraction

- ❖ If dark matter self-interact (e.g., annihilation) via a long range force

- ❖ The cross section could be enhanced for small relative velocities

- ❖ Classical analogue

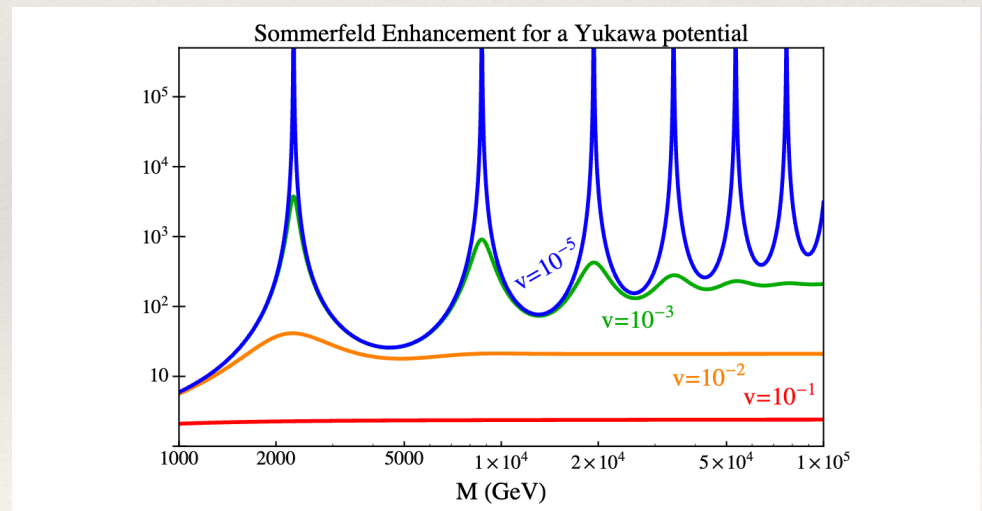
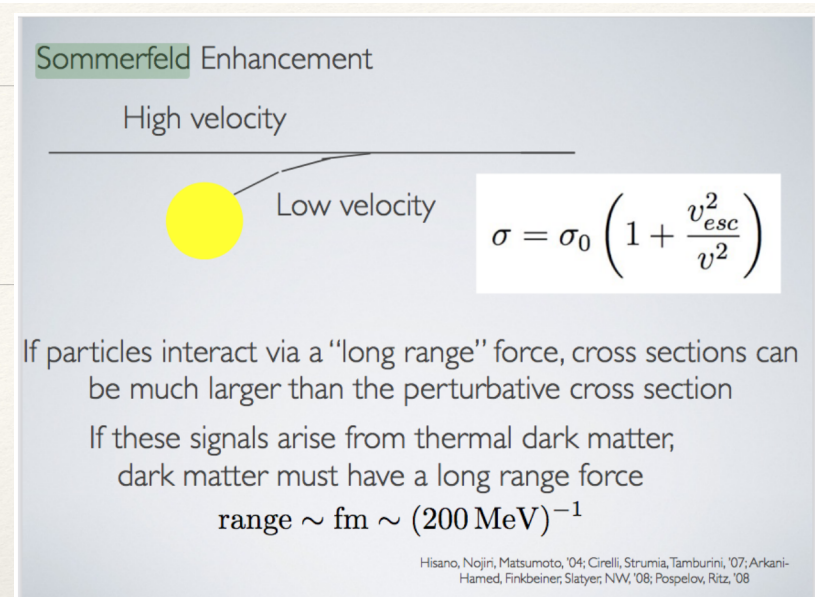
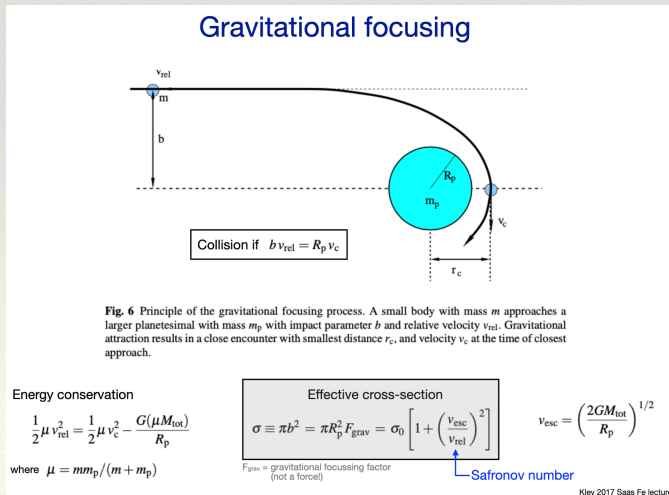


Figure 6: Numerical evaluation of the Sommerfeld enhancement factor as a function of the dark matter reduced mass M for a range of relative velocities. The mediator mass is fixed to 90 GeV and $\alpha = 1/30$.

Back to WIMPs

- ❖ Status of WIMPs
- ❖ Recall that the WIMP prediction was on total cross section
- ❖ If we consider dark matter annihilation into visible channels (not neutrinos)
- ❖ And take the weakest limit
 - ❖ Model agnostic
- ❖ There is still a window open

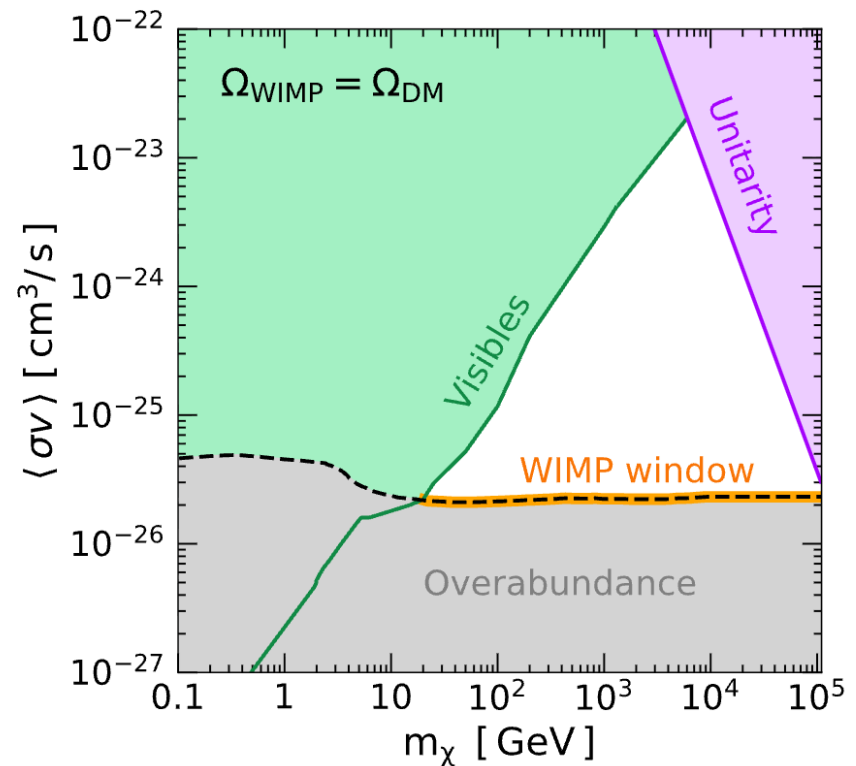


FIG. 9: Bounds on the generic thermal WIMP window (s -wave $2 \rightarrow 2$ annihilation, standard cosmological history), assuming WIMP DM is 100% of the DM. Shown is the conservative bound calculated in this work from data (Visibles), and the unitarity bound [50]. The remaining WIMP window is the orange line, and the white space is unprobed. Thermal relic cross section is the dashed line [4].

Dark Matter annihilation to neutrinos

- ❖ The status of dark matter annihilation into neutrinos
- ❖ If dark matter only take to neutrinos, then WIMPs are far from being tested!

